

# Interrelation between the isoscalar octupole phonon and the proton-neutron mixed-symmetry quadrupole phonon in near spherical nuclei

Nadya A. Smirnova<sup>1,2,3</sup>, Norbert Pietralla<sup>4,5</sup>, Takahiro Mizusaki<sup>6</sup>, Piet Van Isacker<sup>1</sup>

<sup>1</sup> *GANIL, BP 5027, F-14076, Caen Cedex 5, France*

<sup>2</sup> *Centre de Spectrométrie Nucléaire et de Spectrométrie de Masse, F-91405, Orsay, France*

<sup>3</sup> *Institute for Nuclear Physics, Moscow State University, 119899 Moscow, Russia*

<sup>4</sup> *Institut für Kernphysik, Universität zu Köln, 50937 Köln, Germany*

<sup>5</sup> *Wright Nuclear Structure Laboratory, Yale University, New Haven, Connecticut 06520*

<sup>6</sup> *Department of Physics, University of Tokyo, Hongo, Bunkyo-ku, Tokyo 113-0033, Japan*

## Abstract

The interrelation between the octupole phonon and the low-lying proton-neutron mixed-symmetry quadrupole phonon in near-spherical nuclei is investigated. The one-phonon states decay by collective  $E3$  and  $E2$  transitions to the ground state and by relatively strong  $E1$  and  $M1$  transitions to the isoscalar  $2_1^+$  state. We apply the proton–neutron version of the Interacting Boson Model including quadrupole and octupole bosons (*sdf*-IBM-2). Two  $F$ -spin symmetric dynamical symmetry limits of the model, namely the vibrational and the  $\gamma$ -unstable ones, are considered. We derive analytical formulae for excitation energies as well as  $B(E1)$ ,  $B(M1)$ ,  $B(E2)$ , and  $B(E3)$  values for a number of transitions between low-lying states. The model well reproduces many known transition strengths in the near spherical nuclei  $^{142}\text{Ce}$  and  $^{94}\text{Mo}$ .

## I. INTRODUCTION

The phonon concept is a useful and simple concept in nuclear structure physics [1]. The low-lying collective  $J^\pi = 2^+$  and  $3^-$  excitations in near-spherical nuclei can be considered as quadrupole and octupole vibrations, which represent the most important vibrational degrees of freedom at low energies. The bosonic phonon concept suggests the occurrence of multiphonon states, which can decay collectively to states with one phonon less by the annihilation of one phonon. In a harmonic picture  $n$ -phonon states have excitation energies of  $n$  times the one-phonon energy.

Multiphonon and two-phonon states are at present a very actively investigated topic in nuclear structure physics. A two-quadrupole-phonon ( $2^+ \otimes 2^+$ ) triplet with states having spin and parity quantum numbers  $J^\pi = 0^+, 2^+, 4^+$  is usually known in near spherical nuclei. The absence of  $J^\pi = 1^+, 3^+$  members of this two-phonon multiplet points at the bosonic character of the identical quadrupole phonons involved. Multi-quadrupole-phonon states (with  $n > 2$ ) have also been identified, see e.g. [2–4]. The investigation and identification of double giant dipole resonances (2GDR), ( $3^- \otimes 3^-$ ) double-octupole states and ( $2_\gamma^+ \otimes 2_\gamma^+$ )

double-gamma-vibrations in deformed nuclei are actively debated in the literature, see e.g. Refs. [5–11].

The mixed-multipolarity ( $2^+ \otimes 3^-$ ) quadrupole-octupole coupled quintuplet [12,13] with spin and parity quantum numbers  $J^\pi = 1^- - 5^-$  is a very interesting example of the coupling of two different phonons. Members of the ( $2^+ \otimes 3^-$ ) two-phonon quintuplet should decay by definition by collective  $E2$  and  $E3$  transitions to the  $3_1^-$  octupole phonon state and to the  $2_1^+$  quadrupole phonon state, respectively. The ( $2^+ \otimes 3^-$ ) two-phonon states are expected to occur close to the sum energy  $E_{2^+ \otimes 3^-} = E(2_1^+) + E(3_1^-)$ . There are only a few examples, e.g.  $^{144}\text{Sm}$  [14],  $^{144}\text{Nd}$  [15],  $^{142}\text{Ce}$  [16] and  $^{112}\text{Cd}$  [17], where besides the two-phonon  $1^-$  state other multiplet members have been identified experimentally. The reason might be that all the other states from the  $2^+ \otimes 3^-$  quintuplet, except the  $1^-$ , are strongly mixed with non-collective excitations, losing their pure quadrupole–octupole nature. This is supported by shell-model calculations performed recently for  $N = 82$  nuclei [18]. Thus, the most valuable data, which can be used as a testing ground for the concept of quadrupole-octupole coupled two-phonon excitations, are the transition strengths from the  $1^-$  member of the quintuplet.

The  $J^\pi = 1^-$  two-phonon state has been very well investigated in magic and near spherical nuclei. In many nuclei, it has been identified close to the sum energy  $E_{2^+ \otimes 3^-}$ , indicating a quite harmonic phonon coupling [19–21]. According to its definition, the two-phonon  $1^-$  state should decay by a collective one-phonon  $E2$  transition to the  $3^-$  octupole phonon state. This has been confirmed experimentally [22,23]. The collective  $1_{2^+ \otimes 3^-}^- \rightarrow 2_1^+$   $E3$  transition has not yet been measured due to the possibly dominating  $E1$  and  $M2$  contaminations in this transition. A particularly interesting feature of the two-phonon  $1^-$  state is the existence of a relatively strong  $E1$  transition to the ground state, which can be sensitively measured in photon scattering experiments [24]. The strength of this two-phonon annihilating  $E1$  transition approximately equals the strength of the  $3_1^- \rightarrow 2_1^+$  two-phonon changing  $E1$  transition [25].

All the low-energy one-phonon and two-phonon states mentioned above involve isoscalar phonons. Recently the isovector quadrupole excitation in the valence shell, the  $2_{\text{ms}}^+$  state, has been identified in some nuclei from the measurement of absolute transition strengths, see, e.g., [16,26–31]. Isovector excitations in the valence shell form a whole class of low-lying collective states called, more precisely, mixed-symmetry states [32–34]. The fundamental  $2_{\text{ms}}^+$  state decays by a weakly collective  $E2$  transition to the ground state and by a strong  $M1$  transition to the isoscalar  $2_1^+$  state, with an  $M1$  matrix element of the order of one nuclear magneton [34,35]. In an harmonic phonon coupling scheme one can expect also the existence of mixed-symmetry two-phonon multiplets, that involve at least one excitation of the mixed-symmetry quadrupole phonon. A symmetric–mixed-symmetric ( $2_1^+ \otimes 2_{\text{ms}}^+$ ) two-quadrupole phonon excitation with positive parity, namely a  $J^\pi = 1^+$  state (the so-called scissors mode), has been identified already in the near spherical nucleus  $^{94}\text{Mo}$  [31]. Similarly one can expect the existence of a ( $2_{\text{ms}}^+ \otimes 3^-$ ) mixed-symmetry quadrupole-octupole coupled multiplet with negative parity. In a naive phonon coupling picture members of this quintuplet should show a very complex but, nevertheless, simple to understand decay pattern, which can be predicted from the decay properties of the one-phonon excitations (weakly-collective  $E2$  decay and strong  $M1$  decay of the  $2_{\text{ms}}^+$  state, and collective  $E3$  and relatively strong  $E1$  decay of the  $3_1^-$  octupole vibration). For instance, the  $J^\pi = 1_{2_{\text{ms}}^+ \otimes 3^-}^-$  state should decay by relatively strong  $E1$ , strong  $M1$ , weakly-collective  $E2$ , and collective  $E3$  transitions to the ground and to the

$1^+$  scissors state, to the ordinary, isoscalar ( $2^+ \otimes 3^-$ ) multiplet, and to the one-phonon  $3^-$  and  $2_{\text{ms}}^+$  states, respectively (see Fig. 1).

Recently,  $\gamma$  transitions between the  $3^-$  octupole phonon state and the  $2_{\text{ms}}^+$  state have been observed experimentally [16,36] in near spherical nuclei. For an understanding of these new observations it is necessary to investigate the interrelation of the octupole phonon state and the mixed-symmetry  $2_{\text{ms}}^+$  state theoretically. That is one aim of the present article. Another purpose of this article is the proposal of possible two-phonon states generated by the coupling of the octupole degree of freedom with the proton-neutron degree of freedom and the quantitative investigation of the properties of such constructions.

A convenient and sometimes successful approach to new and complicated physical phenomena is the investigation of symmetries and the algebraic solution of symmetric Hamiltonians. In low-energy nuclear structure physics this task can be achieved by application of the algebraic interacting boson model [37,38]. Since we deal simultaneously with the isoscalar octupole vibration and the isovector quadrupole vibration in the valence shell of near spherical nuclei, we need a model which incorporates them both. We apply for the first time the *sdf*-IBM-2, which considers  $l^\pi = 0^+$  monopole (*s*) bosons,  $l^\pi = 2^+$  quadrupole (*d*) bosons,  $l^\pi = 3^-$  octupole (*f*) bosons, and the proton-neutron ( $\pi - \nu$ ) degree of freedom [32].

In this paper we develop the formalism of the *sdf*-IBM-2 in two particular dynamical symmetry limits relevant for the description of vibrational and  $\gamma$ -unstable nuclei. In section II we discuss the group reduction chains of the *sdf*-IBM-2 and the quantum numbers, which are necessary to classify the eigenstates of the dynamically symmetric Hamiltonians. We derive analytical formulae for  $\gamma$  transition rates. The *E1* transitions are calculated with a two-body operator. Quadrupole-octupole coupled two-body operators have turned out to be essential for the description of *E1* transitions generated by quadrupole-octupole collectivity [39,40,25]. In section III the model is applied to data. Within the framework of the *sdf*-IBM-2 we analyze relevant transitions in the near-spherical nuclei  $^{142}\text{Ce}$  and  $^{94}\text{Mo}$ .

## II. SDF-IBM-2

The building blocks of the *sdf*-IBM-2 are  $2 \times 13$  creation and  $2 \times 13$  annihilation operators

$$b_{\rho lm}^+, b_{\rho lm} \quad (1)$$

where  $\rho = \pi, \nu$ ,  $l = 0, 2, 3$ ,  $m = 0, \pm 1, \dots, \pm l$ , which by definition satisfy standard boson commutation relations:

$$[b_{\rho lm}, b_{\rho' l' m'}^+] = \delta_{\rho\rho'} \delta_{ll'} \delta_{mm'} . \quad (2)$$

The total number of bosons is conserved for a given nucleus, i.e.

$$N = N_\pi + N_\nu = n_{s\pi} + n_{d\pi} + n_{f\pi} + n_{s\nu} + n_{d\nu} + n_{f\nu} . \quad (3)$$

The integers  $n_{l\rho}$  in Eq. (3) are the eigenvalues of the boson number operators  $\hat{n}_{l\rho} = (b_{\rho l}^+ \cdot \tilde{b}_{\rho l})$ , where the dot denotes the scalar product and  $\tilde{b}_{\rho l m} = (-1)^{l-m} b_{\rho l, -m}$ .

The  $2 \times 13^2 = 338$  bilinear combinations of proton and neutron boson operators of the type

$$b_{\rho lm}^+ b_{\rho' l' m'} \quad (4)$$

generate the Lie algebra  $U_\pi(13) \otimes U_\nu(13)$ .

## A. Group reductions, quantum numbers and wave functions

The  $U_\pi(13) \otimes U_\nu(13)$  symmetry algebra has a rich substructure. In the present study we are interested in the  $F$ -spin symmetric dynamical symmetry limits of the model, which can be characterized by the reduction chains

$$\begin{array}{ccccccccccc}
 U_\pi(13) \otimes U_\nu(13) & \supset & U_{\pi\nu}(13) & \supset & U_{\pi\nu}(6) \otimes U_{\pi\nu}(7) & \supset & \dots & \supset & SO_{\pi\nu}^d(3) \otimes SO_{\pi\nu}^f(3) & \supset & SO_{\pi\nu}(3) \\
 \downarrow & & \downarrow \\
 [N_\pi] & & [N_\nu] & & [N_1, N_2] & & [n_1, n_2] & & [m_1, m_2] & & \dots & & L_d & & L_f & & L
 \end{array} \tag{5}$$

where the dots denote alternative group reductions discussed later. Below each group we indicate the quantum numbers, associated with it. In total, the complete classification of the basis states (5) requires 26 quantum numbers corresponding to the  $2 \times 13$  occupation numbers  $n_{\rho lm}$  in the  $m$ -scheme. The  $F$ -spin quantum number [32,38] relates in terms of Young tableaux to the one- or two-rowed  $U_{\pi\nu}(13)$  representation as

$$F = \frac{N_1 - N_2}{2}.$$

The maximum value of the  $F$ -spin quantum number

$$F_{\max} = \frac{N}{2}$$

corresponds to the totally symmetric representations of the  $U_{\pi\nu}(13)$  group. States with smaller  $F$ -spin quantum numbers  $F < F_{\max}$  are called mixed-symmetry states and correspond to non-symmetric representations of the  $U_{\pi\nu}(13)$  group. Since the *sd**f*-IBM-2 contains an octupole degree of freedom, it enlarges the diversity of mixed-symmetry states compared to the standard *sd*-IBM-2. This fact can be recognized from the branching rules of  $U_{\pi\nu}(13) \supset U_{\pi\nu}(6) \otimes U_{\pi\nu}(7)$  (see Appendix A).

The simplest two-rowed representation of  $U_{\pi\nu}(13)$  reduces to the  $U_{\pi\nu}(6) \supset U_{\pi\nu}(7)$  representations in the following way:

$$\begin{aligned}
 U_{\pi\nu}(13) & \supset U_{\pi\nu}(6) \otimes U_{\pi\nu}(7) \\
 [N - 1, 1] & = [n - 1, 1] \otimes [m]
 \end{aligned} \tag{6.1}$$

$$[n] \otimes [m - 1, 1] \tag{6.2}$$

$$[n] \otimes [m] \tag{6.3}$$

where,  $n = n_1 + n_2$  is the total number of  $s$  and  $d$  bosons,  $m = m_1 + m_2$  is the number of  $f$  bosons, giving thus  $N = n + m$ .

As follows from Eq. (6), three types of the mixed-symmetry states arise.

1. The  $[n - 1, 1] \otimes [m]$  decomposition corresponds to the usual mixed-symmetry states in the *sd*-space, coupled to  $m$  octupole-bosons with a wave function, which is symmetric in the  $f$ -sector. Examples are the fundamental  $2_{\text{ms}}^+$  state and the  $1_{\text{sc}}^+$  “scissors” state with no  $f$ -boson at all, which belong to the  $U_{\pi\nu}(6) \otimes U_{\pi\nu}(7)$  representation  $[n - 1, 1] \otimes$

[0], or the new negative-parity mixed-symmetry two-phonon states which we denote as  $(2_{\text{ms}}^+ \otimes 3_1^-)$  because they are generated by the coupling of the lowest  $2_{\text{ms}}^+$  state in the  $sd$ -sector and one symmetric  $f$ -boson, which belong to the  $U_{\pi\nu}(6) \otimes U_{\pi\nu}(7)$  representation  $[n-1, 1] \otimes [1]$ . Note that in the presence of one  $f$ -boson due to the boson number conservation only  $n = N - 1$  bosons remain in the  $sd$ -sector, which can belong to the symmetric  $U_{\pi\nu}(6)$  representation  $[n] = [N - 1]$  or to the mixed-symmetry representations, i.e., to the lowest  $[n-1, 1] = [N - 2, 1]$ . Therefore, the representation  $[n-1, 1] \otimes [1]$  can be considered as  $(2_{\text{ms}}^+ \otimes 3_1^-)$  two-phonon states. It turns out from the application of the branching rules given in Appendix A that this  $(2_{\text{ms}}^+ \otimes 3_1^-)$  two-phonon coupling will generate mixed-symmetry states with  $F$ -spin quantum numbers  $F = F_{\text{max}} - 1$  and  $F = F_{\text{max}} - 2$ , because the representation  $[N - 2, 1] \otimes [1]$  is also present in the  $U_{\pi\nu}(13)$  representation  $[N - 2, 2]$ , which has a total  $F$ -spin quantum number  $F = F_{\text{max}} - 2$ . In this article, we restrict ourselves to mixed-symmetry states with  $F = F_{\text{max}} - 1$ .

2. The  $[n] \otimes [m - 1, 1]$  reduction describes the mixed-symmetry states which appear due to mixed-symmetry in the  $f$ -sector. We will not consider such kind of states in the present paper.
3. Finally,  $[n] \otimes [m]$  states are symmetric separately in the  $sd$ - and in the  $f$ -sectors, however, they are coupled in a non-symmetric way within the full  $sd$ -space. The simplest example for a mixed-symmetry state of this type is the  $3_{\text{ms}}^-$  state, which consists of  $m = 1$   $f$ -boson and  $n = N - 1$   $s$ -bosons. This  $3_{\text{ms}}^-$  state is the mixed-symmetry analogue state of the symmetric octupole phonon, the  $3_1^-$  state. This can be clearly seen from the explicit wave functions given in Table IV. Higher excited mixed-symmetry states of this type can be obtained by replacing in a symmetric way  $s$ -bosons with  $d$ -bosons in the  $3_{\text{ms}}^-$  wave function along with proper normalization. We denote the lowest energy example of such mixed-symmetry states schematically as  $(2^+ \otimes 3_{\text{ms}}^-)$ .

The operator which controls the excitation energy of mixed-symmetry states with  $F$ -spin quantum numbers  $F < F_{\text{max}}$  is the Majorana operator. By definition, this is the most general operator which annihilates any totally symmetric state. Within the  $U_{\pi\nu}(13) \supset U_{\pi\nu}(6) \otimes U_{\pi\nu}(7)$ , there are three important types of Majorana operators.

The well known Majorana operator  $\hat{M}_6$  [32] is associated with the  $U(6)$  group generated by the  $s$ - and  $d$ -bosons only. It has the form

$$\hat{M}_6 = [s_\nu^+ \times d_\pi^+ - s_\pi^+ \times d_\nu^+]^{(2)} \cdot [s_\nu \times \tilde{d}_\pi - s_\pi \times \tilde{d}_\nu]^{(2)} - 2 \sum_{k=1,3} [d_\nu^+ \times d_\pi^+]^{(k)} \cdot [\tilde{d}_\nu \times \tilde{d}_\pi]^{(k)}, \quad (7)$$

which influences the states whose wave functions are non-symmetric in the  $sd$ -sector of the model space. In Eq. (7) and below,  $\times$  denotes the standard tensor product of two irreducible tensorial operators. It relates to the  $U_{\pi\nu}(6)$  quadratic Casimir operator as

$$C_2[U_{\pi\nu}(6)] = n(n + 5) - 2\hat{M}_6. \quad (8)$$

The Majorana operator  $\hat{M}_7$  is associated with the  $U(7)$  group generated by the  $f$ -bosons only. It has the form

$$\hat{M}_7 = -2 \sum_{k=1,3,5} [f_\nu^+ \times f_\pi^+]^{(k)} \cdot [\tilde{f}_\nu \times \tilde{f}_\pi]^{(k)} \quad (9)$$

which is responsible for pushing up the mixed-symmetry states of the second type, i.e non-symmetric in the  $f$ -sector. It relates to the  $U_{\pi\nu}(7)$  quadratic Casimir invariant as

$$C_2[U_{\pi\nu}(7)] = m(m+6) - 2\hat{M}_7. \quad (10)$$

Finally, the Majorana operator which is associated with the full group  $U(13)$ , reads

$$\hat{M}_{13} = \hat{M}_6 + \hat{M}_7 + [s_\nu^+ \times f_\pi^+ - s_\pi^+ \times f_\nu^+]^{(3)} \cdot [s_\nu \times \tilde{f}_\pi - s_\pi \times \tilde{f}_\nu]^{(3)} \quad (11)$$

$$+ \sum_{k=1,2,3,4,5} (-1)^{k+1} [d_\nu^+ \times f_\pi^+ - d_\pi^+ \times f_\nu^+]^{(k)} \cdot [d_\nu \times \tilde{f}_\pi - d_\pi \times \tilde{f}_\nu]^{(k)}, \quad (12)$$

$$= [F_{\max}(F_{\max} + 1) - \hat{F}^2]. \quad (13)$$

This operator acts on all three types of mixed-symmetry states.  $\hat{M}_{13}$  relates to the  $U_{\pi\nu}(13)$  quadratic Casimir operator as

$$C_2[U_{\pi\nu}(13)] = N(N+12) - 2\hat{M}_{13}. \quad (14)$$

The most general Hamiltonian constructed from linear and quadratic Casimir operators of the group  $U_{\pi\nu}(6) \otimes U_{\pi\nu}(7)$  reads

$$\begin{aligned} H = & H_0 + \lambda\hat{M}_{13} + \lambda'\hat{M}_6 + \lambda''\hat{M}_7 + \epsilon_d C_1[U_{\pi\nu}(5)] + \alpha C_2[U_{\pi\nu}(5)] + \kappa' C_2[SU_{\pi\nu}(3)] \\ & + \eta C_2[SO_{\pi\nu}(6)] + \beta C_2[SO_{\pi\nu}(5)] + \gamma_d C_2[SO_{\pi\nu}^d(3)] + \epsilon_f C_1[U_{\pi\nu}(7)] \\ & + \kappa C_2[SO_{\pi\nu}(7)] + \xi C_2[G_{2\pi\nu}] + \gamma_f C_2[SO_{\pi\nu}^f(3)] + \gamma C_2[SO_{\pi\nu}(3)]. \end{aligned} \quad (15)$$

The definitions of the Casimir invariants of Lie groups used here are given in Appendix B. The structure of the Majorana operators has interesting consequences. The  $sdf$ -IBM-2 reduces to the simpler version  $sdf$ -IBM-1, if the strength constant  $\lambda$  of the Majorana operator  $\hat{M}_{13}$  is set to infinity. Using a finite value of  $\lambda$ , but  $\lambda'' = \infty$  will remove only those states which have mixed-symmetry in the  $f$ -sector alone. We will use this choice throughout the paper. For the ordinary mixed-symmetry states in the  $sd$ -sector, which are known already from the  $sd$ -IBM-2, the sum  $\lambda + \lambda'$  plays the role of the ordinary Majorana parameter in the  $sd$ -IBM-2. The excitation energies of mixed-symmetry states, which contain one  $f$ -boson are in addition also functions of the quantity  $\lambda - \lambda'$ . This parameter controls the excitation energy of mixed-symmetry states with negative parity.

Since we are going to study vibrational or  $\gamma$ -unstable nuclei, we are interested in two well-known dynamical symmetry limits of the positive parity  $sd$ -subchain [38], namely,

$$U_{\pi\nu}(6) \supset \left\{ \begin{array}{l} U_{\pi\nu}(5) \\ SO_{\pi\nu}(6) \end{array} \right\} \supset SO_{\pi\nu}(5) \supset SO_{\pi\nu}(3) \quad (16)$$

which we consider in the following subsections.

The negative parity subchain has a unique reduction [41,42]:

$$\begin{array}{ccccccc} U_{\pi\nu}(7) & \supset & SO_{\pi\nu}(7) & \supset & G_{2\pi\nu} & \supset & SO_{\pi\nu}(3) \\ \downarrow & & \downarrow & & \downarrow & & \downarrow \\ [m_1, m_2] & & (\omega_1, \omega_2) & & (u_1, u_2) & & \{\beta_j\} \quad L_f \end{array} \quad (17)$$

where the quantum numbers  $\{\beta_j\}$  ( $j = 1, 2, 3, 4$ ) are the so-called missing labels, which are necessary to classify completely the  $G_2 \supset SO(3)$  reduction. Unlike the case of  $sdf$ -IBM-1 where only the totally symmetric representations are important [37,42], we also deal here with two-rowed representations of the algebras in (5) and (17). This requires some modifications. For example, we have to take into account the exceptional group  $G_2$ . For the reduction of not fully symmetric representations of  $SO(7)$  the group  $G_2$  helps to resolve the labelling problem. The missing label, which is in general necessary to uniquely define the  $SO(7) \supset G_2$  reduction, is redundant in our case of only two-rowed representations.

1. The  $U_{\pi\nu}(1) \otimes U_{\pi\nu}(5) \otimes U_{\pi\nu}(7)$  dynamical symmetry limit

In this dynamical symmetry limit the reduction chain of the positive parity  $U_{\pi\nu}(6)$  sub-algebra is [38]

$$\begin{array}{ccccccc}
U_{\pi\nu}(6) & \supset & U_{\pi\nu}(5) & \supset & SO_{\pi\nu}(5) & \supset & SO_{\pi\nu}^d(3) \\
\downarrow & & \downarrow & & \downarrow & & \downarrow \\
[n_1, n_2] & & \{n_{d_1}, n_{d_2}\} & & [\tau_1, \tau_2] & & \{\alpha_i\} L_d
\end{array} \tag{18}$$

where  $\alpha_i$  ( $i = 1, 2$ ) are missing labels, necessary to completely classify the  $SO(5) \supset SO(3)$  reduction. We denote here  $n = n_1 + n_2$  the total number of  $s$  and  $d$  bosons, while the number of  $d$  bosons only is denoted as  $n_d = n_{d_1} + n_{d_2}$ . Thus, the total wave function can be written as

$$|[N_\pi] \otimes [N_\nu]; [N_1, N_2][n_1, n_2]\{n_{d_1}, n_{d_2}\}(\tau_1, \tau_2)\{\alpha_i\}L_d; [m_1, m_2](\omega_1, \omega_2)(u_1, u_2)\{\beta_j\}L_f; LM] \tag{19}$$

The quantum numbers of the lowest states are given in Table I.

In the  $U_{\pi\nu}(5) \otimes U_{\pi\nu}(7)$  dynamical symmetry limit it is rather simple to construct explicitly the wave functions. We shall do this in order to make clear the variety of mixed-symmetry states appearing in the model. In Table I we present the wave functions for some states of interest. We discussed above already the one- $f$ -boson octupole states. Of particular interest are here also the lowest  $1^-$  states. From the coupling of one  $d$ -boson quadrupole phonon and one  $f$ -boson octupole phonon four  $1^-$  states emerge. This is evident in the  $m$ -scheme in  $F$ -space because the four basis wave functions  $|d_\pi f_\pi\rangle$ ,  $|d_\nu f_\pi\rangle$ ,  $|d_\pi f_\nu\rangle$ , and  $|d_\nu f_\nu\rangle$  can be formed. These basis states can be combined to states with  $U_{\pi\nu}(13)$  symmetry and good  $F$ -spin. One obtains one symmetric  $1^-$  state corresponding to the totally symmetric  $[N]$  irrep of  $U_{\pi\nu}(13)$  with  $F$ -spin quantum number  $F = F_{\max}$ , and three mixed-symmetry states: two of them with  $F$ -spin quantum numbers  $F = F_{\max} - 1$  and one with  $F = F_{\max} - 2$ . One  $F = F_{\max} - 1$  state corresponds to the  $[N - 1, 1] \supset [N - 2, 1] \otimes [1]$  reduction and the other to the  $[N - 1, 1] \supset [N - 1] \otimes [1]$  reduction in the  $U_{\pi\nu}(13) \supset U_{\pi\nu}(6) \otimes U_{\pi\nu}(7)$ , chain. The last one arises from the  $[N - 2, 2] \supset [N - 2, 1] \otimes [1]$  reduction. According to the discussion above we denote them as  $1^- = (2^+ \otimes 3^-)_{1^-}$ ,  $1_{ms}^- = (2_{ms}^+ \otimes 3^-)_{1^-}$ ,  $1_{ms}'^- = (2^+ \otimes 3_{ms}^-)_{1^-}$  and  $1_{ms}''^-$ , respectively.

The  $U_{\pi\nu}(5) \otimes U_{\pi\nu}(7)$  dynamical symmetry Hamiltonian expressed in terms of Casimir invariants of first and second order of the relevant groups reads

$$\begin{aligned}
H = & H_0 + \lambda \hat{M}_{13} + \lambda' \hat{M}_6 + \lambda'' \hat{M}_7 + \epsilon_d C_1[\text{U}_{\pi\nu}(5)] \\
& + \alpha C_2[\text{U}_{\pi\nu}(5)] + \beta C_2[\text{SO}_{\pi\nu}(5)] + \gamma_d C_2[\text{SO}_{\pi\nu}^d(3)] + \epsilon_f C_1[\text{U}_{\pi\nu}(7)] \\
& + \kappa C_2[\text{SO}_{\pi\nu}(7)] + \xi C_2[\text{G}_{2\pi\nu}] + \gamma_f C_2[\text{SO}_{\pi\nu}^f(3)] + \gamma C_2[\text{SO}_{\pi\nu}(3)] .
\end{aligned} \tag{20}$$

The eigenvalue problem for the dynamical symmetry Hamiltonian (20) can be solved analytically. The solution of the full U(5) Hamiltonian reads

$$\begin{aligned}
E = & E_0 + \lambda [F_{\max}(F_{\max} + 1) - F(F + 1)] + \lambda' n_2(n_1 + 1) + \lambda'' m_2(m_1 + 1) \\
& + \epsilon_d(n_{d_1} + n_{d_2}) + \alpha[n_{d_1}(n_{d_1} + 4) + n_{d_2}(n_{d_2} + 2)] + \beta[\tau_1(\tau_1 + 3) + \tau_2(\tau_2 + 1)] \\
& + \gamma_d L_d(L_d + 1) + \epsilon_f(m_1 + m_2) + \kappa[\omega_1(\omega_1 + 5) + \omega_2(\omega_2 + 3)] \\
& + \xi[u_1(u_1 + 5) + u_2(u_2 + 4) + u_1 u_2] + \gamma_f L_f(L_f + 1) + \gamma L(L + 1) .
\end{aligned} \tag{21}$$

To construct the spectrum one needs to know the branching rules for the groups involved (see Appendix). An energy spectrum corresponding to (20) is shown in Fig. 2. The parameters of the Hamiltonian are specified in the figure caption.

## 2. The $\text{SO}_{\pi\nu}(6) \otimes \text{U}_{\pi\nu}(7)$ dynamical symmetry limit

In this dynamical symmetry limit the reduction chain of the positive parity  $\text{U}_{\pi\nu}(6)$  sub-algebra is

$$\begin{array}{ccccccc}
\text{U}_{\pi\nu}(6) & \supset & \text{SO}_{\pi\nu}(6) & \supset & \text{SO}_{\pi\nu}(5) & \supset & \text{SO}_{\pi\nu}^d(3) \\
\downarrow & & \downarrow & & \downarrow & & \downarrow \\
[n_1, n_2] & & \langle \sigma_1, \sigma_2 \rangle & & [\tau_1, \tau_2] & & \{ \alpha_i \} \quad L_d
\end{array} \tag{22}$$

and the total wave function is as follows:

$$|[N_\pi] \otimes [N_\nu]; [N_1, N_2][n_1, n_2] \langle \sigma_1, \sigma_2 \rangle (\tau_1, \tau_2) \{ \alpha_i \} L_d; [m_1, m_2] (\omega_1, \omega_2) (u_1, u_2) \{ \beta_j \} L_f; LM \rangle \tag{23}$$

The quantum numbers for the lowest states in this dynamical symmetry are presented in Table II.

The  $\text{SO}_{\pi\nu}(6) \otimes \text{U}_{\pi\nu}(7)$  dynamical symmetry Hamiltonian reads

$$\begin{aligned}
H = & H_0 + \lambda \hat{M}_{13} + \lambda' \hat{M}_6 + \lambda'' \hat{M}_7 + \zeta C_2[\text{SO}_{\pi\nu}(6)] \\
& + \beta C_2[\text{SO}_{\pi\nu}(5)] + \gamma_d C_2[\text{SO}_{\pi\nu}^d(3)] + \epsilon_f C_1[\text{U}_{\pi\nu}(7)] \\
& + \kappa C_2[\text{SO}_{\pi\nu}(7)] + \xi C_2[\text{G}_{2\pi\nu}] + \gamma_f C_2[\text{SO}_{\pi\nu}^f(3)] + \gamma C_2[\text{SO}_{\pi\nu}(3)] .
\end{aligned} \tag{24}$$

and has the eigenvalues

$$\begin{aligned}
E = & E_0 + \lambda [F_{\max}(F_{\max} + 1) - F(F + 1)] + \lambda' n_2(n_1 + 1) + \lambda'' m_2(m_1 + 1) \\
& + \zeta[\sigma_1(\sigma_1 + 4) + \sigma_2(\sigma_2 + 2)] + \beta[\tau_1(\tau_1 + 3) + \tau_2(\tau_2 + 1)] + \gamma_d L_d(L_d + 1) \\
& + \epsilon_f(m_1 + m_2) + \kappa[\omega_1(\omega_1 + 5) + \omega_2(\omega_2 + 3)] \\
& + \xi[u_1(u_1 + 5) + u_2(u_2 + 4) + u_1 u_2] + \gamma_f L_f(L_f + 1) + \gamma L(L + 1) .
\end{aligned} \tag{25}$$

The branching rules for the corresponding groups can be found in Ref. [52] and in the Appendix below. A typical energy spectrum corresponding to Eq. (25) is shown in Fig. 3. The parameters are specified in the caption.

## B. Electromagnetic transitions

In this subsection we discuss electromagnetic transitions between low-lying states in the *sd**f*-IBM-2 with particular emphasis of those transitions which are new in the present model with respect to the standard *sd*-IBM-2 and *sd**f*-IBM-1 species. For the study of the interrelation between the  $F = F_{\max}$  octupole phonon and the  $F = F_{\max} - 1$  mixed-symmetry quadrupole phonon and possible two-phonon states generated by the coupling of them, we are interested in  $E1$ ,  $M1$ ,  $E2$ , and  $E3$  transition strengths. The reduced transition probabilities

$$B(\Pi\lambda; J_i \rightarrow J_f) = \frac{1}{2J_i + 1} |\langle J_f || T(\Pi\lambda) || J_i \rangle|^2 \quad (26)$$

are calculated from the matrix elements of the transition operators  $T(\Pi\lambda)$ , where  $\Pi$  stands for the radiation character, either  $E$  or  $M$ , and  $\lambda$  denotes the multipolarity.

The electric quadrupole operator reads

$$T(E2) = e_\pi Q_\pi^{(2)} + e_\nu Q_\nu^{(2)} , \quad (27)$$

where

$$Q_\rho^{(2)} = [d_\rho^+ \times s_\rho + s_\rho^+ \times \tilde{d}_\rho]^{(2)} + \chi_\rho [d_\rho^+ \times \tilde{d}_\rho]^{(2)} + \chi'_\rho [f_\rho^+ \times \tilde{f}_\rho]^{(2)} . \quad (28)$$

The magnetic dipole operator has the form

$$T(M1) = \sqrt{\frac{3}{4\pi}} (g_\pi L_\pi^d + g_\nu L_\nu^d + g'_\pi L_\pi^f + g'_\nu L_\nu^f) , \quad (29)$$

where

$$L_\rho^d = \sqrt{10} [d_\rho^+ \times \tilde{d}_\rho]^{(1)} , \quad L_\rho^f = 2\sqrt{7} [f_\rho^+ \times \tilde{f}_\rho]^{(1)} . \quad (30)$$

According to the Eqs. (27–30) the addition of the  $f$  boson enlarges the structure of electromagnetic operators of the standard *sd*-IBM-2. The standard *sd*-IBM-2, however, works well for the description of  $E2$  and  $M1$  transitions. In order to reduce the number of model parameters in the *sd**f*-IBM-2 we, therefore, neglect below those parts of the  $E2$  and  $M1$  transition operators which involve the  $f$ -boson. Thus, we assume  $\chi'_\rho = 0$  and  $g'_\rho = 0$ . In contrast, the  $f$ -boson is essential for  $E3$  and  $E1$  transitions, which are new with respect to the *sd*-IBM-2.

Since there is at present no experimental evidence for the existence of states with mixed-symmetry in the  $f$ -boson sector, we shall consider here only  $F$ -scalar octupole transitions, i.e., we use the following symmetric octupole operator:

$$T(E3) = e_3 (O_\pi^{(3)} + O_\nu^{(3)}) , \quad (31)$$

where  $O_\rho^{(3)}$  stands for

$$O_\rho^{(3)} = [s_\rho^+ \times \tilde{f}_\rho + f_\rho^+ \times s_\rho]^{(3)} + \chi [d_\rho^+ \times \tilde{f}_\rho + f_\rho^+ \times \tilde{d}_\rho]^{(3)} . \quad (32)$$

The general one-body electric dipole operator has the form

$$T(E1) = \alpha_\pi D_\pi^{(1)} + \alpha_\nu D_\nu^{(1)}, \quad (33)$$

where

$$D_\rho^{(1)} = [d_\rho^+ \times \tilde{f}_\rho + f_\rho^+ \times \tilde{d}_\rho]^{(1)}. \quad (34)$$

While the one-body  $M1$ ,  $E2$ , and  $E3$  transition operators work satisfactorily, the one-body  $E1$ -transition operator fails to provide an adequate description of dipole transition strengths in vibrational nuclei [39]. The operator (33) has very strict selection rules, conserving the total number of  $d$ - and  $f$ -bosons  $\Delta(n_d + n_f) = 0$ . This contradicts the experimental findings where the quadrupole-octupole collective  $E1$  transitions, including the ground state decay of the quadrupole-octupole two-phonon  $1^-$  state, are even found to be enhanced, see e.g. Refs. [19–21,24].

Two approaches exist to avoid this problem. Following the first, the  $sdf$ -IBM is enlarged with a  $p$  boson ( $l^\pi = 1^-$ ), thus leading to the so-called  $spdf$ -IBM [44–47]. The inclusion of the  $p$  boson in the IBM corresponds to the consideration of a collective dipole vibration. The  $p$  boson induced one-body electric dipole operator works successfully for the description of dipole transition strengths in deformed nuclei [44–49]. For near-spherical nuclei the  $p$  boson does not help much to eliminate all discrepancies [17]. Moreover, the ground state transition of the lowest  $1^-$  state can be understood only if this state is identified with the collective negative-parity dipole mode, which would render the agreement of its excitation energy with the quadrupole-octupole two-phonon sum energy a sheer coincidence. Therefore, another approach is preferable.

A multiphonon structure of excitations in vibrational nuclei as well as an octupole or quadrupole-octupole coupled origin of negative-parity states, naturally suggests an  $E1$ -transition operator which contains a quadrupole-octupole coupled two-body part. Such a picture is also supported by the empirical correlation between  $E1$ -transition strengths of the  $1_1^- \rightarrow 0_1^+$  and  $3_1^- \rightarrow 2_1^+$  transitions found recently for heavy near-spherical nuclei [25] and by microscopic calculations [50].

The two-body dipole operator has already been introduced within the simple quadrupole and octupole phonon model [25] as well as within the  $sdf$ -IBM [40,51]. This ansatz is in good agreement with the available data. The  $E1$  transition operator considered here has the form

$$T(E1) = \alpha_\pi D_\pi^{(1)} + \alpha_\nu D_\nu^{(1)} + \frac{\beta}{2N} \left[ (Q_\pi^{(2)} + \eta Q_\nu^{(2)}) \times (O_\pi^{(3)} + O_\nu^{(3)}) + (O_\pi^{(3)} + O_\nu^{(3)}) \times (Q_\pi^{(2)} + \eta Q_\nu^{(2)}) \right]^{(1)}, \quad (35)$$

where  $D_\rho^{(1)}$ ,  $Q_\rho^{(2)}$ , and  $O_\rho^{(3)}$  are given by the Eqs. (34), (28) with  $\chi'_\rho = 0$ , and (32), respectively, and  $\eta = e_\nu/e_\pi$ . We stress that we introduce only one free parameter more ( $\beta$ ) in the  $E1$  operator with respect to the one-body operator from Eq. (33). Below we analyze  $E1$ -transitions within two particular dynamical symmetry limits and we apply the results in section III to the description of data on the near-spherical nuclei  $^{142}\text{Ce}$  and  $^{94}\text{Mo}$ .

1. The  $U_{\pi\nu}(1)\otimes U_{\pi\nu}(5)\otimes U_{\pi\nu}(7)$  dynamical symmetry limit

Using the wave functions (19) we can obtain the matrix elements of the transition operators (27), (29), (31) and (35). The technique for the calculation of such matrix elements is described in detail in Ref. [52]. In this particular dynamical symmetry limit, it is more convenient to use the explicit expressions of the wave functions constructed from boson operators following the method described in [53] (see, e.g., Ref. [52]). The  $E2$  and  $M1$  transition strengths between those states, whose wave functions do not involve any  $f$  bosons, are exactly the same as in the case of the  $sd$ -IBM-2 and can be found in [52]. The advantage of the  $sd$ -IBM-2 is that it provides the description of  $E2$  and  $M1$  transitions between negative parity states and of  $E1$  and  $E3$  transitions between the states of different parity and different  $F$ -spin. Here we are particularly interested in the electric dipole transitions which connect the octupole  $3_1^-$  state with the symmetric  $2_1^+$  state and with the mixed-symmetry  $2_{ms}^+$  state, as well as in those which connect the  $(2^+ \otimes 3^-)$  two-phonon negative parity multiplet with the ground state band. We also consider here the new mixed-symmetry quadrupole-octupole coupled dipole states  $1_{ms}^- = (2_{ms}^+ \otimes 3^-)_{1-}$  and  $1_{ms}'^- = (2^+ \otimes 3_{ms}^-)_{1-}$  and their electromagnetic properties (including  $M1$  strengths) as examples for mixed-symmetry states with negative parity. Analytical expressions of reduced transition probabilities are summarized in Table III.

It is worthwhile to look closely to the analytical expressions in Table III in order to recognize the fingerprints of the simple phonon picture the consideration of which has guided us to the present model. The  $E1$  transition strengths from the  $3_1^-$  state to the symmetric and mixed-symmetry one-phonon quadrupole excitations, the  $2_1^+$  state and the  $2_{ms}^+$  state, are both of the order of  $(1/N)^0$ , i.e., they can be strong on an absolute scale and comparable. The  $3_1^- \rightarrow 2_{ms}^+$   $F$ -vector  $E1$  strength can be even larger than that of the strong  $F$ -scalar  $3_1^- \rightarrow 2_1^+$   $E1$  transition if the effective electric dipole charges  $\alpha_\pi$  and  $\alpha_\nu$  have opposite signs. Similarly, the  $E1$  ground state excitation strengths to the  $1_1^-$  state and the  $1_{ms}^-$  state are both of the order of  $(1/N)^0$  due to the two-body part of the  $E1$  operator. However, here the  $F$ -scalar  $0_1^+ \rightarrow 1_1^-$   $E1$  strength must be expected to be larger than the  $F$ -vector  $E1$  strength of the  $0_1^+ \rightarrow 1_{ms}^-$  transition because the parameter  $\eta$  usually takes values between 0 and 1 leading to a reduction of the  $F$ -vector  $E1$  strength which is proportional to the factor  $(1 - \eta)^2$ . It is also interesting to compare the properties of the new mixed-symmetry  $1^-$  states,  $1_{ms}^-$  and  $1_{ms}'^-$ . The direct  $E1$  ground state excitation strengths to the  $1_{ms}'^-$  state is only of the order of  $(1/N)^2$  and therefore much smaller than the  $E1$  strength to the  $1_{ms}^-$  state, which is of the order of  $(1/N)^0$ . The  $1_{ms}^- \rightarrow 3_1^-$   $E2$  strength is of the order of  $N$ , which indicates quadrupole collectivity. Since it is proportional to the square of the difference of the effective quadrupole boson charges  $(e_\pi - e_\nu)^2$  this transition should be weakly collective like the known  $2_{ms}^+ \rightarrow 0_1^+$  one-quadrupole phonon decay. In contrast, the  $1_{ms}'^- \rightarrow 3_1^-$   $E2$  strength is of the order of  $1/N$  and cannot be large. Very interesting are also the  $M1$  transitions between symmetric and mixed-symmetry negative parity states. The  $M1$  strengths from the  $1_{ms}^-$  state to the quadrupole-octupole coupled  $1^-$  and  $2^-$  two-phonon states are of the order of  $(1/N)^0$  and should be comparable to the  $2_{ms}^+ \rightarrow 2_1^+$  strong  $M1$  transition. The  $1_{ms}'^- \rightarrow 1^-, 2^-$   $M1$  transitions are of the order of  $(1/N)^2$  if the  $d$ -boson part alone is used in the  $M1$  transition operator (29). If one allows for finite  $g$ -factors  $g'_\rho$  for the  $f$ -boson parts in the  $M1$  operator (29), they will be responsible for the leading term of the order of

$(1/N)^0$  which was therefore included in Table III. This resembles the fact that the  $1_{\text{ms}}^-$  state originates from the non symmetric coupling of an  $f$ -boson to the  $sd$ -sector. In summary the  $1_{\text{ms}}^-$  state shows the behavior, which is mentioned in the introduction to be expected for a two-phonon state formed by the coupling of the fundamental phonons which generate the  $3_1^-$  state and the  $2_{\text{ms}}^+$  state.

### 2. The $SO_{\pi\nu}(6)\otimes U_{\pi\nu}(7)$ dynamical symmetry limit

Using the wave functions (23) we have calculated the matrix elements of the transition operators (27), (29), (31) and (35). We use here the quadrupole operator (28) with  $\chi_\rho = 0$  as is conventional for the  $SO(6)$  limit. The analytical expressions for the  $E2$  and  $M1$  transitions between the states which are formed only from  $s$  and  $d$  bosons are identical to those of the  $sd$ -IBM-2 and can be found in Ref. [52]. Analytical expressions for  $E2$  and  $M1$  transition strengths between negative parity states and for  $E1$  and  $E3$  transition strengths are summarized in Table IV.

## III. COMPARISON WITH EXPERIMENT

In this section we apply the  $sd$ *f*-IBM-2 to electromagnetic transitions between states of the near spherical nuclei  $^{94}\text{Mo}$  and  $^{142}\text{Ce}$ . In both nuclei the “key-states” of the  $sd$ *f*-IBM-2 are known: the quadrupole and octupole phonon states, fragments of the mixed-symmetry  $2_{\text{ms}}^+$  state, and members of the symmetric ( $2^+ \otimes 3^-$ ) two-phonon multiplet [16,26,31,54,55]. Moreover,  $\gamma$ -transition strengths between the  $3^-$  state and the  $2_{\text{ms}}^+$  state have been measured [16,36]. Up to now these are the only examples of such transitions. The near-spherical nuclei  $^{142}\text{Ce}$  and  $^{94}\text{Mo}$  were considered before as reasonable examples for the schematic, but analytically solvable,  $U(5)$  and  $O(6)$  dynamical symmetry limits of the IBM [31,56]. We will first discuss transition strengths in the nucleus  $^{142}\text{Ce}$  in terms of the  $U(5)$  dynamical symmetry limit of the  $sd$ *f*-IBM-2 and we apply then the  $O(6)$  dynamical symmetry limit of the  $sd$ *f*-IBM-2 to transition strengths in the nucleus  $^{94}\text{Mo}$ .

### A. $^{142}\text{Ce}$

The quadrupole properties and enhanced  $M1$  transitions in some  $N = 84$  isotones have been studied within the standard IBM-2 by Hamilton *et al.* [56] and within both the IBM-2 and a particle-core coupling model by Copnell *et al.* [57]. The experimental data on the dipole and octupole electromagnetic transition strengths taken from Refs. [16,26,54] can be found in Table V.

The symmetric quadrupole phonon  $2_1^+$  state lies at an excitation energy of  $E(2_1^+) = 641$  keV and the  $3^-$  octupole phonon state is low-lying at  $E(3^-) = 1653$  keV. The  $1^-$  member of the symmetric ( $2^+ \otimes 3^-$ ) quadrupole-octupole coupled two-phonon multiplet has a short lifetime of  $\tau(1^-) = 16(3)$  fs. It lies at an excitation energy of  $E(1^-) = 2188$  keV, which is close to the sum energy  $E(2_1^+) + E(3^-) = 2294$  keV of the constituent phonons. This  $1^-$  state decays by enhanced electric dipole transitions to the ground state and to the  $2_1^+$  state

with relatively large  $E1$  strengths of the order of  $10^{-3} e^2\text{fm}^2$ . A rather strong  $E2$  transition to the  $3_1^-$  state is in agreement with the measurement [16].

$^{142}\text{Ce}$  is one of the few nuclei for which, besides the  $1^-$  state, data on other members of the  $(2^+ \otimes 3^-)$  quintuplet is known. Based on the data of their neutron-scattering experiment Vanhoy *et al.* [16] assigned the  $5_1^-$  state at 2125 keV and the  $4_1^-$  state at 2385 keV to be of quadrupole-octupole coupled nature. These states are characterized by strong  $E2$  transitions to the one-phonon octupole state and rather strong  $E1$  transitions to the ground state band. The assignment of  $2^-$  and  $3^-$  two-phonon states is less clear. The reason may be possible stronger mixing with noncollective configurations. Two candidates were previously considered [16] to have notable collective two-phonon components, the  $2^{(-)}$  state at 2728 keV and the state at 2768 keV with ambiguous spin assignment  $J = (1 - 3)$ .

A fragment of the  $2_{\text{ms}}^+$  state, namely the  $2_3^+$  state at 2005 keV excitation energy, has been identified by Hamilton *et al.* [56]. Large  $E2$  and  $M1$  transition strengths have been firstly measured for that state in a Coulomb excitation experiment by Vermeer *et al.* [26] and corrected to slightly lower values in the more precise experiment by Vanhoy *et al.* [16]. This state decays, furthermore, by a relatively strong  $E1$  transition to the  $3^-$  octupole phonon state with a reduced transition strength of [16]

$$B(E1; 2_3^+ \rightarrow 3^-) = 4.6(5) \times 10^{-3} e^2\text{fm}^2, \quad (36)$$

which is remarkably large. This large  $E1$  transition strength between a fragment of the  $2_{\text{ms}}^+$  state and the  $3_1^-$  octupole phonon state represents to our knowledge the first absolute value for the strength of an  $F$ -vector  $E1$  transition. However, the  $(n, n'\gamma)$  data by Vanhoy *et al.* [16], suggest the short-lived  $2_4^+$  state at 2365 keV excitation energy as another fragment of the  $2_{\text{ms}}^+$  state of  $^{142}\text{Ce}$  from its strong  $M1$  transition to the  $2_1^+$  state. Therefore, it is not yet clear whether the  $B(E1)$  value (36) represents the total  $F$ -vector  $2_{\text{ms}}^+ \rightarrow 3^-$   $E1$  strength or whether it is only a part of it.

It is the purpose of the following subsection to show that it is reasonable to apply the proposed scheme for electromagnetic transitions between states of the  $sd\text{f}$ -IBM-2 to the nucleus  $^{142}\text{Ce}$  and to find appropriate parameters of the  $E3$  and  $E1$  transition operators for this nucleus. To minimize the set of model parameters, which we must determine from data, we use literature values for such parameters which were determined already. For the description of  $E2$  transitions in  $^{142}\text{Ce}$ , we choose here the parameters found by Hamilton *et al.* in an earlier  $sd$ -IBM-2 study [56]:  $e_\pi = 12 e \text{fm}^2$ ,  $e_\nu = 24 e \text{fm}^2$ ,  $\chi_\pi = 0$ ,  $\chi_\nu = -1.3$ . Despite the unusual feature that the neutron quadrupole charge factor is larger than the proton one, this parameter set matches the data on  $E2$  transition strengths and the quadrupole moment of the  $2_1^+$  state well (see discussions in Ref. [56,26]). For the  $M1$  transition operator we use bare orbital values for the boson  $g$ -factors,  $g_\pi = 1 \mu_N$  and  $g_\nu = 0$  without any parameter adjustment. The octupole charge factor  $e_3$  has been determined from the  $B(E3; 0_1^+ \rightarrow 3_1^-)$  value. It is  $e_3 = 76 e \text{fm}^3$ . The structural parameter  $\chi$  in the  $E3$  transition operator cannot be fixed from hitherto measured  $E3$  strengths. Its value will be determined below from measured quadrupole-octupole induced  $E1$  transition strengths, which are sensitive to it. To establish the three parameters of the  $E1$  transition operator and the parameter  $\chi$  of the  $E3$  operator, we take four electric dipole transitions as given, namely  $B(E1; 3_1^- \rightarrow 2_1^+)$ ,  $B(E1; 3_1^- \rightarrow 2_{\text{ms}}^+)$ ,  $B(E1; 1_1^- \rightarrow 0_1^+)$  and  $B(E1; 1_1^- \rightarrow 2_1^+)$ . While the three last values for  $^{142}\text{Ce}$  are known to be of the order  $10^{-3} e^2\text{fm}^2$ , for the first one

only a small upper limit is established [16]. We use the reasonable estimate  $B(E1; 3_1^- \rightarrow 2_1^+) = 1 \times 10^{-4} e^2 \text{fm}^2$ . As a solution of the set of four quadratic equations in the four parameters  $\chi$ ,  $\beta$ ,  $\alpha_\pi$ ,  $\alpha_\nu$ , we get in general eight different parameter sets, if we neglect an overall sign, which is relevant for electric dipole moments only. All these parameter sets have the same  $|\beta| = 0.058 e \text{ fm}$ , two possible values of  $\chi$ , 7.04 and  $-6.75$ , and 4 possible choices of  $\alpha_\rho$  for each value of  $\chi$ . To select an appropriate parameter set, one has to check the consistency with data on other transitions, which have a different functional dependence of the parameters. In our case an unambiguous selection of the best parameter set was not possible. We use here two different sets which provide also a relative good description of the other known dipole transition strengths.

In Table V we present the  $E1$ -transition rates calculated for the two sets of parameters:  $\beta = 0.058 e \text{ fm}$ ,  $\chi = -6.75$ ,  $\alpha_\pi = -0.081 e \text{ fm}$ ,  $\alpha_\nu = 0.0012 e \text{ fm}$  (Theory I) and  $\beta = 0.058 e \text{ fm}$ ,  $\chi = 7.04$ ,  $\alpha_\pi = -0.111 e \text{ fm}$ ,  $\alpha_\nu = 0.143 e \text{ fm}$  (Theory II). Some comments are necessary.

- Although the observed strength of the  $3_1^- \rightarrow 2_1^+$   $E1$ -transition is unexpectedly small, it can be described simultaneously with the enhanced  $E1$ -transitions from the  $1_1^-$  state to the ground state and to the  $2_1^+$  state.
- The large  $B(E1)$  value for the transition from  $3_1^-$  state to  $2_2^+$  is predicted while this transition was not observed at all. The reason may be that since  $E_\gamma(3_1^- \rightarrow 2_2^+) = 115.5 \text{ keV}$ , its intensity is much smaller than that of the  $3_1^- \rightarrow 4_1^+$  transition with  $E_\gamma = 433.5 \text{ keV}$  ( $I \sim E_\gamma^3 B(E1)$ ) and, therefore, escaped observation.
- The  $B(E1; 4_1^- \rightarrow 3_1^+)$  value is remarkably large in agreement with the model. This transition strength was not used to fit the parameters of the transition operator.
- The  $B(E1; 5_1^- \rightarrow 4_1^+, 6_1^+)$  values are relatively small in agreement with the model.
- The transition from  $3_1^-$  state to  $3_1^+$  is still outside the model, even if we apply the two-body dipole operator. This interesting selection rule may be exploited to analyze a possible breaking of the assumed symmetries [ $F$ -spin or  $U(5)$ ].

Another interesting group of excited states which we can discuss in the framework of the *sdf*-IBM-2 is the group of mixed-symmetry states with negative parity. The relatively low-lying quintuplet of states, denoted by  $(2_{\text{ms}}^+ \otimes 3^-)$  is of the most interest, because both constituent phonons are already known experimentally. In a naive phonon coupling scheme one may expect this quintuplet to exist approximately at the sum-energy of the constituent phonons, which is  $E(2_{\text{ms}}^+) + E(3^-) \approx 3.8 \text{ MeV}$  for  $^{142}\text{Ce}$ . In this energy region the mixing of the collective states with non-collective excitations can be expected to be already rather strong. Supposing that  $1^-$  states are well spaced and less mixed, we will consider only these states here and we include the *sdf*-IBM-2 predictions for the decay strengths of mixed-symmetry  $1^-$  states in Table V. We stress that  $E1$  excitation strengths  $B(E1; 0_1^+ \rightarrow 1^-) = 3 \times B(E1; 1^- \rightarrow 0_1^+) \approx 1 \times 10^{-3} e^2 \text{fm}^2$  as it is predicted for the  $1_{\text{ms}}^-$  state can be well detected in highly sensitive photon scattering experiments like those which are performed in Stuttgart [24] or in Darmstadt [58].

## B. $^{94}\text{Mo}$

$^{94}\text{Mo}$  is another near-spherical nucleus, for which data on the most relevant states for the *sdf*-IBM-2 is known. The  $E2$  and  $E3$  excitation strengths to the quadrupole and octupole phonon states, the  $2_1^+$  state at 871 keV and the  $3_1^-$  state at 2534 keV, are known from Coulomb excitation experiments [59]. The quadrupole-octupole coupled  $J^\pi = 1^-$  two-phonon state has recently been identified at an excitation energy of 3260 keV in a photon scattering experiment [55]. The one-phonon and two-phonon positive parity mixed-symmetry states, the  $2_3^+$  state at 2068 keV and the  $1_1^+$  state at 3129 keV, could be assigned from the measurement of large  $M1$  transition strengths [31]. There exists the most complete set of data for these  $1_{\text{ms}}^+, 2_{\text{ms}}^+$  mixed-symmetry states in  $^{94}\text{Mo}$  due to the new combination of a photon scattering experiment and  $\gamma\gamma$ -coincidence studies following  $\beta$ -decay. The measurement [31] agrees with a collective  $1_{\text{ms}}^+ \rightarrow 2_{\text{ms}}^+$   $E2$  transition supporting the two-phonon character of the  $1_{\text{ms}}^+$  state. Particularly interesting for the present study in the framework of the *sdf*-IBM-2 is the observation of a  $\gamma$  transition between the  $3_1^-$  isoscalar octupole phonon state and the  $2_3^+$  mixed-symmetry quadrupole phonon state. The branching ratio

$$\frac{B(E1; 3_1^- \rightarrow 2_{\text{ms}}^+)}{B(E1; 3_1^- \rightarrow 2_1^+)} = 14(2) \quad (37)$$

is known and remarkably large. Besides the data on  $^{142}\text{Ce}$  this branching ratio in  $^{94}\text{Mo}$  represents further evidence for the possible dominance of  $F$ -vector  $E1$  transitions over  $F$ -scalar  $E1$ -transitions. We stress that  $F$ -vector  $E1$  transitions can be treated within the framework of the *sdf*-IBM-2, while they are outside the scope of hitherto considered versions of the IBM, such as *sd*-IBM-2, *sdf*-IBM-1 or *spdf*-IBM-1. The  $3_1^-$  state has recently been investigated in a  $^{91}\text{Zr}(\alpha, n)^{94}\text{Mo}$  experiment in Cologne. From the measured line shapes, the branching ratios, and the known  $E3$  excitation strength the  $3^-$  lifetime could be estimated to be  $\tau \approx 2$  ps resulting however in relatively wide ranges for the absolute values of the  $E1$  decay strengths, which are given in Table VI.

$E2$  and  $M1$  transition strengths in  $^{94}\text{Mo}$  were satisfactorily reproduced previously in the  $O(6)$  dynamical symmetry limit of the *sd*-IBM-2 with a minimum set of free parameters in the transition operators [31]. We apply here the  $O(6)$  limit of the *sdf*-IBM-2 to additionally describe  $E1$  and  $E3$  strengths in  $^{94}\text{Mo}$ .

For the electric quadrupole operator we use for simplicity the schematic parameters proposed in Ref. [31], namely,  $e_\pi = 9 e \text{ fm}^2$ ,  $e_\nu = 0 e \text{ fm}^2$ ,  $\chi_\pi = \chi_\nu = 0$ . We take here  $\chi_\rho = 0$ , because this choice is usual for the  $O(6)$  limit. In fact, experimental  $B(E2)$  values, which are sensitive to the  $\chi_\rho$  parameters are about two orders of magnitude smaller than the  $B(E2; 2_1^+ \rightarrow 0_1^+)$  value. Another argument for the use of the parameter values  $\chi_\rho = 0$  can be deduced from the validity of the  $d$ -parity selection rules [60] for the nucleus  $^{94}\text{Mo}$ . The  $d$ -parity refers to the symmetry of IBM basis states with respect to the change of sign of the  $d$ -boson. From this symmetry it follows that the  $1_1^+ \rightarrow 2_1^+$   $M1$  transition strength almost vanishes. This is actually observed in  $^{94}\text{Mo}$ . Consequently, the terms in the Hamiltonian, which violate the  $d$ -parity must be small. In the usually adopted consistent  $Q$  formalism of the IBM the only terms which violate the  $d$ -parity symmetry of the Hamiltonian are those proportional to  $\chi_\rho$  [60]. The deduced small  $d$ -parity violation results in small values for the parameters  $\chi_\rho$  supporting the choice  $\chi_\rho = 0$ , which we adopt from Ref. [31]. From the

measured [31]  $E2$  excitation strengths to the symmetric one-quadrupole-phonon excitation, the  $2_1^+$  state, and the mixed-symmetry one-quadrupole-phonon excitation, the  $2_{\text{ms}}^+$  state, the ratio  $|\eta| = |e_\nu/e_\pi| \approx 0.1$  can be deduced for  $^{94}\text{Mo}$  if  $^{100}\text{Sn}$  is used as the inert core. Therefore, the value  $\eta = 0$  was used for the schematic description of  $E2$  transition strengths in the  $sd$ -IBM-2 in Ref. [31]. We adopt here this parameter value without further adjustment.  $M1$  transition strengths are described by using bare orbital values for the boson  $g$ -factors  $g_\pi = 1 \mu_N$  and  $g_\nu = 0$  and  $g'_\rho = 0$ . From the measured  $B(E3; 0_1^+ \rightarrow 3_1^-)$  value we can determine the octupole charge factor  $e_3 = 51.5 e \text{ fm}^3$ . From four known transitions we can determine a set of parameters in the electric dipole operator. The  $B(E1)$  values calculated with the parameter set

$$\alpha_\pi = -0.039 e \text{ fm} , \alpha_\nu = 0.074 e \text{ fm} , \beta = 0.035 e \text{ fm} , \chi = 3.45 , \quad (38)$$

are shown in Table VI. Unfortunately no other relevant  $E1$  transition strength is known in  $^{94}\text{Mo}$  to check the predictive power of the  $sdf$ -IBM-2 approach with respect to  $E1$  transitions as was possible for  $^{142}\text{Ce}$ . It is worthwhile to mention that some predictions of the IBM-2 concerning positive parity mixed-symmetry states with spin quantum numbers  $J > 2$  could very recently be verified in  $^{94}\text{Mo}$  by the discovery of a  $3_{\text{ms}}^+$  state in Cologne [61]. This observation gives further confidence in the concept of mixed-symmetry states.

#### IV. SUMMARY

The relation and coupling of the collective octupole degree of freedom to proton-neutron mixed-symmetry states is discussed in the framework of the interacting boson model. For this purpose  $s$ -bosons,  $d$ -bosons, and  $f$ -bosons as well as the proton-neutron degree of freedom had to be taken into account leading to the hitherto not considered  $sdf$ -IBM-2 version of the model. We developed the formalism of the  $sdf$ -IBM-2 and considered two  $F$ -spin symmetric dynamical symmetry limits denoted by  $U_{\pi\nu}(1) \otimes U_{\pi\nu}(5) \otimes U_{\pi\nu}(7)$  and  $SO_{\pi\nu}(6) \otimes U_{\pi\nu}(7)$ . These analytically solvable limits of the model are relevant for the description of near spherical, vibrational and  $\gamma$ -unstable nuclei, respectively. The full dynamically symmetric Hamiltonians are formulated, their eigenstates are specified and the analytical expressions for their excitation energies are given. Low-lying, collective, negative parity states are discussed including for the first time negative parity mixed-symmetry states. Analytical expressions for  $E1$ ,  $M1$ ,  $E2$ , and  $E3$  transition strengths were evaluated. The  $E1$  operator considered here contains a quadrupole-octupole coupled two-body part besides the one-body term. The model has been applied to two near spherical nuclei,  $^{142}\text{Ce}$  and  $^{94}\text{Mo}$ , for which some states are known, which are particularly relevant for the  $sdf$ -IBM-2. Several electromagnetic transition strengths, including  $B(E1)$  values, are well reproduced by the  $sdf$ -IBM-2. Evidence for the possible dominance of  $F$ -vector  $E1$  transitions over  $F$ -scalar  $E1$  transitions is found. The decay properties of  $1_{\text{ms}}^-$  states in the nucleus  $^{142}\text{Ce}$  are predicted.

#### ACKNOWLEDGMENTS

We thank C. Fransen for informing us about transition strengths in  $^{94}\text{Mo}$  prior to publication. We gratefully acknowledge discussions with P. von Brentano, R. F. Casten, C. Fransen,

A. Gelberg, F. Iachello, J. Jolie, R. V. Jolos, T. Otsuka, A. Wolf, and A. Zilges. The paper is supported partly by the Competitive Center at the St. Petersburg State University, and by the Deutsche Forschungsgemeinschaft under Contracts No. Br 799/9-1 and Pi 393/1-1. N.A.S., N.P. and P.V.I. thank the Institute for Nuclear Theory, University of Washington for hospitality. This work was partially supported by the U.S. DOE under Contract No. DE-FG02-91ER-40609 and by Grant-in-Aid for Scientific Research (B)(2)(10044059) from the Ministry of Education, Science and Culture.

## APPENDIX A: $U(13) \supset U(6) \otimes U(7)$ BRANCHING RULES

In order to provide a complete classification scheme we need to reduce the representations of  $U(13)$  group to the Kronecker product  $U(6) \otimes U(7)$ . Here we present the branching rules only for the totally symmetric  $[N]$  and the lowest mixed-symmetry  $[N-1, 1]$  and  $[N-2, 2]$  irreducible representations of  $U(13)$ . The  $U(6) \otimes U(7)$  representations are denoted as  $[\alpha] \otimes [\beta]$ . Those  $U(6) \otimes U(7)$  decompositions, which contain  $1^-$  states discussed in the text, are underlined.

$$\begin{aligned}
[N] &= [N] \otimes [0], \underline{[N-1] \otimes [1]}, \dots, [1] \otimes [N-1], [0] \otimes [N] \\
[N-1, 1] &= [N-1, 1] \otimes [0], \underline{[N-2, 1] \otimes [1]}, \dots, [2, 1] \otimes [N-3], [1, 1] \otimes [N-2] \\
&\quad \underline{[N-1] \otimes [1]}, \underline{[N-2] \otimes [2]}, \dots, [2] \otimes [N-2], [1] \otimes [N-1] \\
&\quad \underline{[N-2] \otimes [1, 1]}, [N-3] \otimes [2, 1], \dots, [1] \otimes [N-2, 1], [0] \otimes [N-1, 1] \\
[N-2, 2] &= [N-2, 2] \otimes [0], [N-3, 2] \otimes [1], \dots, [3, 2] \otimes [N-5], [2, 2] \otimes [N-4] \\
&\quad \underline{[N-2, 1] \otimes [1]}, \underline{[N-3, 1] \otimes [2]}, \dots, [3, 1] \otimes [N-4], [2, 1] \otimes [N-3] \\
&\quad \underline{[N-2] \otimes [2]}, \underline{[N-3] \otimes [3]}, \dots, [3] \otimes [N-3], [2] \otimes [N-2] \\
&\quad [N-3, 1] \otimes [1, 1], [N-4, 1] \otimes [2, 1], \dots, [2, 1] \otimes [N-4, 1], [1, 1] \otimes [N-3, 1] \\
&\quad [N-3] \otimes [2, 1], [N-4] \otimes [3, 1], \dots, [2] \otimes [N-3, 1], [1] \otimes [N-2, 1] \\
&\quad [N-4] \otimes [2, 2], [N-5] \otimes [3, 2], \dots, [1] \otimes [N-3, 2], [0] \otimes [N-2, 2]
\end{aligned} \tag{A1}$$

The branching rules for the chains  $U(6) \supset U(5) \supset SO(5) \supset SO(3)$  and  $U(6) \supset SO(6) \supset SO(5) \supset SO(3)$  reduction chains can be found elsewhere [38]. The partial classification scheme for the chain  $U(7) \supset SO(7) \supset G_2 \supset SO(3)$  is given in Table VII.

## APPENDIX B: CASIMIR INVARIANTS

The Casimir invariants of Lie algebras exploited here can be expressed in terms of boson creation and annihilation operators as follows [38]:

$$\begin{aligned}
C_1 [\text{U}(7)] &= (f^+ \cdot \tilde{f}) , \\
C_2 [\text{U}(7)] &= \sum_{K=0}^6 [f^+ \times \tilde{f}]^{(K)} \cdot [f^+ \times \tilde{f}]^{(K)} , \\
C_1 [\text{U}(6)] &= (s^+ \cdot s) + (d^+ \cdot \tilde{d}) , \\
C_2 [\text{U}(6)] &= (s^+ \cdot s) \cdot (s^+ \cdot s) + \sum_{K=0}^4 [d^+ \times \tilde{d}]^{(K)} \cdot [d^+ \times \tilde{d}]^{(K)} , \\
C_2 [\text{SU}(3)] &= 2 \left( [d^+ \times s + s^+ \times \tilde{d}]^{(2)} - \frac{\sqrt{7}}{2} [d^+ \times \tilde{d}]^{(2)} \right) \left( [d^+ \times s + s^+ \times \tilde{d}]^{(2)} - \frac{\sqrt{7}}{2} [d^+ \times \tilde{d}]^{(2)} \right) \\
&\quad + \frac{15}{2} [d^+ \times \tilde{d}]^{(1)} \cdot [d^+ \times \tilde{d}]^{(1)} , \\
C_2 [\text{SO}(7)] &= \sum_{K=1,3,5,7} [f^+ \times \tilde{f}]^{(K)} \cdot [f^+ \times \tilde{f}]^{(K)} , \\
C_2 [\text{SO}(6)] &= [d^+ \times s + s^+ \times \tilde{d}]^{(2)} \cdot [d^+ \times s + s^+ \times \tilde{d}]^{(2)} + 2 \sum_{K=1,3} [d^+ \times \tilde{d}]^{(K)} \cdot [d^+ \times \tilde{d}]^{(K)} , \\
C_2 [\text{SO}(5)] &= \sum_{K=1,3} [d^+ \times \tilde{d}]^{(K)} \cdot [d^+ \times \tilde{d}]^{(K)} , \\
C_2 [\text{SO}^d(3)] &= 10 [d^+ \times \tilde{d}]^{(1)} \cdot [d^+ \times \tilde{d}]^{(1)} , \\
C_2 [\text{SO}^f(3)] &= 28 [f^+ \times \tilde{f}]^{(1)} \cdot [f^+ \times \tilde{f}]^{(1)} , \\
C_2 [\text{G}_2] &= \sum_{K=1,5} [f^+ \times \tilde{f}]^{(K)} \cdot [f^+ \times \tilde{f}]^{(K)} .
\end{aligned} \tag{B1}$$

The exceptional algebra  $\text{G}_2$  has been introduced in physics by Racah [41]. The eigenvalues of the Casimir invariants from (B1) in an irreducible representation given by a  $[f_1 f_2 \dots f_n]$  Young tableau are

$$\begin{aligned}
\langle C_1 [\text{U}(n)] \rangle &= \sum_{i=1}^n f_i , \\
\langle C_2 [\text{U}(n)] \rangle &= \sum_{i=1}^n f_i (f_i + n + 1 - 2i) , \\
\langle C_2 [\text{SU}(3)] \rangle &= \lambda^2 + \mu^2 + \lambda\mu + 3\lambda + 3\mu , \quad (\lambda = f_1 - f_2, \mu = f_2) \\
\langle C_2 [\text{SO}(2n+1)] \rangle &= \sum_{i=1}^n 2f_i (f_i + 2n + 1 - 2i) , \\
\langle C_2 [\text{SO}(2n)] \rangle &= \sum_{i=1}^n 2f_i (f_i + 2n - 2i) , \\
\langle C_2 [\text{G}_2] \rangle &= f_1 (f_1 + 5) + f_2 (f_2 + 4) + f_1 f_2 .
\end{aligned} \tag{B2}$$

## REFERENCES

- [1] A. Bohr and B. R. Mottelson, *Nuclear Structure II* (Benjamin, New York, 1975).
- [2] A. Aprahamian, D.S. Brenner, R.F. Casten, R.L. Gill and A. Pietrowski, Phys. Rev. Lett. 59 (1987) 535.
- [3] J. Kern, P.E. Garrett, J. Jolie and H. Lehmann, Nucl. Phys. A 593 (1995) 21.
- [4] R.F. Casten, J. Jolie, H.G. Börner, D.S. Brenner, N.V. Zamfir, W.-T. Chou and A. Aprahamian, Phys. Lett. B 297 (1992) 19; Phys. Lett. B 300 (1993) 411.
- [5] R. Schmidt, Th. Blaich, Th.W. Elze, H. Emling, H. Freiesleben, K. Grimm, W. Henning, R. Holzmann, J.G. Keller, H. Klingler, R. Kulesa, J.V. Kratz, D. Lambrecht, J.S. Lange, Y. Leifels, E. Lubkiewicz, E.F. Moore, E. Wajda, W. Prokopowicz, Ch. Schutter, H. Spies, K. Stelzer, J. Stroth, and W. Walus, H.J. Wollersheim, M. Zinser and E. Zude, Phys. Rev. Lett. 70 (1993) 1767.
- [6] T. Aumann, P.F. Bortignon and H. Emling, Ann. Rev. Nucl. Part. Sci. 48 (1998) 351.
- [7] C. Volpe, Ph. Chomaz, M.V. Andres, F. Catara and E.G. Lanza, Nucl. Phys. A 647 (1999) 246.
- [8] P. Kleinheinz, J. Styczen, M. Piiparinen, J. Blomqvist and M. Kortelahti, Phys. Rev. Lett. 48 (1982) 1457.
- [9] M. Yeh, P.E. Garrett, C.A. McGrath, S.W. Yates and T. Belgya, Phys. Rev. Lett. 76 (1996) 1208.
- [10] H.G. Börner, J. Jolie, S.J. Robinson, B. Krusche, R. Piepenbring, R.F. Casten, A. Aprahamian and J.P. Draayer, Phys. Rev. Lett. 66 (1991) 691.
- [11] P.E. Garrett, M. Kadi, M. Li, C.A. McGrath, V. Sorokin, M. Yeh and S.W. Yates, Phys. Rev. Lett. 78 (1997) 4545.
- [12] P. O. Lipas, Nucl. Phys. 82 (1966) 91.
- [13] P. Vogel and L. Kocbach, Nucl. Phys. A 176 (1971) 33.
- [14] R. A. Gatenby, J. R. Vanhoy, E. M. Baum, E.L. Johnson, S.W. Yates, T. Belgya, B. Fazekas, A. Veres and G. Molnar, Phys. Rev. C 41 (1990) R414.
- [15] S. J. Robinson, J. Jolie, H. G. Börner, P. Schillebeeckx, S. Ulbig and K.P. Lieb, Phys. Rev. Lett. 73 (1994) 412.
- [16] J. R. Vanhoy, J. M. Anthony, B. M. Haas, B.H. Benedict, B.T. Meehan, S.F. Hicks, C.M. Davoren and C.L. Lundstedt, Phys. Rev. C 52 (1995) 2387.
- [17] P. E. Garrett, H. Lehmann, J. Jolie, C.A. McGrath, M. Yeh and S.W. Yates, Phys. Rev. C 59 (1999) 2455.
- [18] L. Esser, R.V. Jolos and P. von Brentano, Nucl. Phys. A 650 (1999) 157.
- [19] F.R. Metzger, Phys. Rev. C 17 (1978) 939.
- [20] R.-D. Herzberg, I. Bauske, P. von Brentano, Th. Eckert, R. Fischer, W. Geiger, U. Kneissl, J. Margraf, H. Maser, N. Pietralla, H.H. Pitz and A. Zilges, Nucl. Phys. A 592 (1995) 211.
- [21] J. Bryssinck, L. Govor, D. Belic, F. Bauwens, O. Beck, P. von Brentano, D. De Frenne, T. Eckert, C. Fransen, K. Govaert, R.-D. Herzberg, E. Jacobs, U. Kneissl, H. Maser, A. Nord, N. Pietralla, H.H. Pitz, V.Yu. Ponomarev and V. Werner, Phys. Rev. C 59 (1999) 1930.
- [22] M. Wilhelm, E. Radermacher, A. Zilges and P. von Brentano, Phys. Rev. C 54 (1996) R449.

- [23] M. Wilhelm, S. Kasemann, G. Pascovici, E. Radermacher, P. von Brentano, and A. Zilges, *Phys. Rev. C* 57 (1998) 577.
- [24] U. Kneissl, H. H. Pitz and A. Zilges, *Prog. Part. Nucl. Phys.* 37 (1996) 349.
- [25] Norbert Pietralla, *Phys. Rev. C* 59 (1999) 2941.
- [26] W. J. Vermeer, C. S. Lim and R. H. Spear, *Phys. Rev. C* 38 (1998) 2982.
- [27] B. Fazekas, T. Belgya, G. Molnar, A. Veres, R.A. Gatenby, S.W. Yates and T. Otsuka, *Nucl. Phys. A* 548 (1992) 249.
- [28] P.E. Garrett, H. Lehmann, C.A. McGrath, Minfang Yeh and S.W. Yates, *Phys. Rev. C* 54 (1996) 2259.
- [29] I. Wiedenhöver, A. Gelberg, T. Otsuka, N. Pietralla, J. Gableske, A. Dewald and P. von Brentano, *Phys. Rev. C* 56 (1997) R2354.
- [30] N. Pietralla, D. Belic, P. von Brentano, C. Fransen, R.-D. Herzberg, U. Kneissl, H. Maser, P. Matschinsky, A. Nord, T. Otsuka, H.H. Pitz, V. Werner and I. Wiedenhöver, *Phys. Rev. C* 58 (1998) 796.
- [31] N. Pietralla, C. Fransen, D. Belic, P. von Brentano, C. Friessner, U. Kneissl, A. Linnemann, A. Nord, H. H. Pitz, T. Otsuka, I. Schneider, V. Werner and I. Wiedenhöver, *Phys. Rev. Lett.* 83 (1999) 1303.
- [32] A. Arima, T. Otsuka, F. Iachello and I. Talmi, *Phys. Lett. B* 66 (1977) 205.
- [33] T. Otsuka, Ph.D. thesis, University of Tokyo, 1978, unpublished.
- [34] F. Iachello, *Phys. Rev. Lett.* 53 (1984) 1427.
- [35] N. Pietralla, C. Fransen, P. von Brentano, C. Friessner, A. Gade, A. Linnemann, P. Matschinsky, I. Schneider, V. Werner, I. Wiedenhöver, D. Belic, U. Kneissl, A. Nord and H. H. Pitz, Contribution to the International Conference on *Nuclear Models 1998*, October, 12 – 14 1998, Camerino, Italy, in press.
- [36] C. Fransen *et al.*, in preparation.
- [37] A. Arima and F. Iachello, *Phys. Rev. Lett.* 35 (1975) 1069.
- [38] F. Iachello and A. Arima, *The Interacting Boson Model* (Cambridge University Press, Cambridge, 1987).
- [39] C. S. Han, D. S. Chuu, S. T. Hsieh and H. C. Chiang, *Phys. Lett. B* 163 (1988) 295.
- [40] A. F. Barfield, P. von Brentano, A. Dewald, K. O. Zell, N. V. Zamfir, D. Bucurescu, M. Ivascu and O. Scholten, *Z. Phys. A* 332 (1989) 29.
- [41] G. Racah, *Phys. Rev.* 76 (1949) 1352.
- [42] S. G. Rohoziński, *J. Phys. G* 4 (1978) 1075.
- [43] B. G. Wybourne, *Symmetry Principles and Atomic Spectroscopy* (Wiley-Interscience, New York, 1970)
- [44] G. Maino, A. Ventura, L. Zuffi and F. Iachello, *Phys. Lett. B* 152 (1985) 17.
- [45] J. Engel and F. Iachello, *Nucl. Phys. A* 472 (1987) 61.
- [46] T. Otsuka and M. Sugita, *Phys. Lett. B* 209 (1988) 140.
- [47] D. F. Kusnezov and F. Iachello, *Phys. Lett. B* 209 (1988) 420.
- [48] M. Sugita, T. Otsuka and P. von Brentano, *Phys. Lett. B* 389 (1996) 642.
- [49] G. L. Long, T. Y. Shen, H. Y. Ji and E. G. Zhao, *Phys. Rev. C* 57 (1998) 2301.
- [50] V. Yu. Ponomarev, *Z. Phys. A*, in press.
- [51] P. von Brentano, N. V. Zamfir and A. Zilges, *Phys. Lett. B* 278 (1992) 221.
- [52] P. Van Isacker, K. Heyde, J. Jolie and A. Sevrin, *Ann. Phys. (N.Y.)* 171 (1986) 253.
- [53] O. Scholten, Ph.D. thesis (1980).

- [54] C. Fransen, O. Beck, P. von Brentano, T. Eckert, R.-D. Herzberg, U. Kneissl, H. Maser, A. Nord, N. Pietralla, H.H. Pitz and A. Zilges, *Phys. Rev. C* 57 (1998) 129.
- [55] N. Pietralla, C. Fransen, P. von Brentano, U. Kneissl and H. H. Pitz, contribution to the *Tenth Symposium on Capture Gamma-Ray Spectroscopy and Related Topics*, (Santa Fe, New Mexico, September 1999), in press.
- [56] W. D. Hamilton, A. Irbäck and J. P. Elliott, *Phys. Rev. Lett.* 53 (1984) 2469.
- [57] J. Copnell, S. J. Robinson, J. Jolie and K. Heyde, *Phys. Rev. C* 46 (1982) 1301.
- [58] P. Mohr, J. Enders, T. Hartmann, H. Kaiser, D. Schiesser, S. Schmitt, S. Volz, F. Wissel and A. Zilges, *Nucl. Instrum. Meth. A* 423 (1999) 480.
- [59] J. Barrette, M. Barrette, A. Boutard, R. Haroutunian, G. Lamoureaux and S. Monaro, *Phys. Rev. C* 6 (1972) 1339.
- [60] N. Pietralla, P. von Brentano, A. Gelberg, T. Otsuka, A. Richter, N. Smirnova and I. Wiedenhöver, *Phys. Rev. C* 58 (1998) 191.
- [61] N. Pietralla, C. Fransen, A. Dewald, C. Frießner, J. Gableske, P. von Brentano, submitted for publication.

TABLES

TABLE I. Notation for some low-lying states in the  $U_{\pi\nu}(1) \otimes U_{\pi\nu}(5) \otimes U_{\pi\nu}(7)$  dynamical symmetry limit.

|                            | $[[N_\pi] \otimes [N_\nu]; [N_1, N_2], [n_1, n_2] \{n_{d_1}, n_{d_2}\} (\tau_1, \tau_2) \{\alpha_i\} L_d; [m_1, m_2] (\omega_1, \omega_2) (u_1, u_2) \{\beta_j\} L_f; L]$   |
|----------------------------|---|
| $ 0_1^+\rangle$            | $=  [N_\pi] \otimes [N_\nu]; [N], [N]\{0\}(0)0; [0](0)(0)0; 0) =  s_\pi^{N_\pi} s_\nu^{N_\nu}; 0)$  |
| $ 0_2^+\rangle$            | $=  [N_\pi] \otimes [N_\nu]; [N], [N]\{2\}(0)0; [0](0)(0)0; 0)$<br>$= (N(N-1))^{-1/2} \left( \sqrt{N_\pi(N_\pi-1)}  d_\pi^2; 0\rangle + \sqrt{2N_\nu N_\pi}  d_\pi d_\nu; 0\rangle + \sqrt{N_\nu(N_\nu-1)}  d_\nu^2; 0\rangle \right)$  |
| $ 1_{\text{ms}}^+\rangle$  | $=  [N_\pi] \otimes [N_\nu]; [N-1, 1], [N-1, 1]\{1, 1\}(1, 1)1; [0](0)(0)0; 1)$<br>$=  d_\pi d_\nu; 1\rangle$   |
| $ 2_1^+\rangle$            | $=  [N_\pi] \otimes [N_\nu]; [N], [N]\{1\}(1)2; [0](0)(0)0; 2)$<br>$= N^{-1/2} (\sqrt{N_\pi}  d_\pi; 2\rangle + \sqrt{N_\nu}  d_\nu; 2\rangle)$   |
| $ 2_2^+\rangle$            | $=  [N_\pi] \otimes [N_\nu]; [N], [N]\{2\}(2)2; [0](0)(0)0; 2)$<br>$= (N(N-1))^{-1/2} \left( \sqrt{N_\pi(N_\pi-1)}  d_\pi^2; 2\rangle + \sqrt{2N_\nu N_\pi}  d_\pi d_\nu; 2\rangle + \sqrt{N_\nu(N_\nu-1)}  d_\nu^2; 2\rangle \right)$  |
| $ 2_{\text{ms}}^+\rangle$  | $=  [N_\pi] \otimes [N_\nu]; [N-1, 1], [N-1, 1]\{1\}(1)2; [0](0)(0)0; 2)$<br>$= N^{-1/2} (\sqrt{N_\nu}  d_\pi; 2\rangle - \sqrt{N_\pi}  d_\nu; 2\rangle)$   |
| $ 3_1^+\rangle$            | $=  [N_\pi] \otimes [N_\nu]; [N], [N]\{3\}(3)3; [0](0)(0)0; 3)$<br>$= (N(N-1)(N-2))^{-1/2} \left( \sqrt{N_\pi(N_\pi-1)(N_\pi-2)}  d_\pi^3; 3\rangle + \sqrt{N_\nu(N_\nu-1)(N_\nu-2)}  d_\nu^3; 3\rangle \right)$<br>$+ \sqrt{3N_\pi(N_\pi-1)N_\nu} \left( \sqrt{\frac{5}{7}}  d_\pi(2)d_\nu; 3\rangle - \sqrt{\frac{2}{7}}  d_\pi(4)d_\nu; 3\rangle \right)$<br>$+ \sqrt{3N_\pi N_\nu(N_\nu-1)} \left( \sqrt{\frac{5}{7}}  d_\nu(2)d_\pi; 3\rangle - \sqrt{\frac{2}{7}}  d_\nu(4)d_\pi; 3\rangle \right)$ |
| $ 3_{\text{ms}}^+\rangle$  | $=  [N_\pi] \otimes [N_\nu]; [N-1, 1], [N-1, 1]\{1, 1\}(1, 1)3; [0](0)(0)0; 3)$<br>$=  d_\pi d_\nu; 3\rangle$   |
| $ 4_1^+\rangle$            | $=  [N_\pi] \otimes [N_\nu]; [N], [N]\{2\}(2)4; [0](0)(0)0; 4)$<br>$= (N(N-1))^{-1/2} \left( \sqrt{N_\pi(N_\pi-1)}  d_\pi^2; 4\rangle + \sqrt{2N_\nu N_\pi}  d_\pi d_\nu; 4\rangle + \sqrt{N_\nu(N_\nu-1)}  d_\nu^2; 4\rangle \right)$  |
| $ 6_1^+\rangle$            | $=  [N_\pi] \otimes [N_\nu]; [N], [N]\{3\}(3)6; [0](0)(0)0; 6)$<br>$= (N(N-1)(N-2))^{-1/2} \left( \sqrt{N_\pi(N_\pi-1)(N_\pi-2)}  d_\pi^3; 6\rangle + \sqrt{N_\nu(N_\nu-1)(N_\nu-2)}  d_\nu^3; 6\rangle \right)$<br>$+ \sqrt{3N_\pi(N_\pi-1)N_\nu} \left( \sqrt{\frac{5}{7}}  d_\pi(2)d_\nu; 6\rangle - \sqrt{\frac{2}{7}}  d_\pi(4)d_\nu; 6\rangle \right)$<br>$+ \sqrt{3N_\pi N_\nu(N_\nu-1)} \left( \sqrt{\frac{5}{7}}  d_\nu(2)d_\pi; 6\rangle - \sqrt{\frac{2}{7}}  d_\nu(4)d_\pi; 6\rangle \right)$ |
| $ 3_1^-\rangle$            | $=  [N_\pi] \otimes [N_\nu]; [N], [N-1]\{0\}(0)0; [1](1)(1)3; 3)$<br>$= N^{-1/2} (\sqrt{N_\pi}  f_\pi; 3\rangle + \sqrt{N_\nu}  f_\nu; 3\rangle)$   |
| $ 3_{\text{ms}}^-\rangle$  | $=  [N_\pi] \otimes [N_\nu]; [N-1, 1], [N-1]\{0\}(0)0; [1](1)(1)3; 3)$<br>$= N^{-1/2} (\sqrt{N_\nu}  f_\pi; 3\rangle - \sqrt{N_\pi}  f_\nu; 3\rangle)$  |
| $ 1_1^-\rangle$            | $=  [N_\pi] \otimes [N_\nu]; [N], [N-1]\{1\}(1)2; [1](1)(1)3; 1)$<br>$= (N(N-1))^{-1/2} \left( \sqrt{N_\pi(N_\pi-1)}  d_\pi f_\pi; 1\rangle + \sqrt{N_\nu(N_\nu-1)}  d_\nu f_\nu; 1\rangle \right)$<br>$+ \sqrt{N_\nu N_\pi}  d_\pi f_\nu; 1\rangle + \sqrt{N_\nu N_\pi}  d_\nu f_\pi; 1\rangle)$   |
| $ 1_{\text{ms}}^-\rangle$  | $=  [N_\pi] \otimes [N_\nu]; [N-1, 1], [N-2, 1]\{1\}(1)2; [1](1)(1)3; 1)$<br>$= ((N-1)(N-2))^{-1/2} \left( \sqrt{N_\nu(N_\pi-1)}  d_\pi f_\pi; 1\rangle - \sqrt{N_\pi(N_\nu-1)}  d_\nu f_\nu; 1\rangle \right)$<br>$+ (N_\nu-1)  d_\pi f_\nu; 1\rangle - (N_\pi-1)  d_\nu f_\pi; 1\rangle)$   |
| $ 1_{\text{ms}}'^-\rangle$ | $=  [N_\pi] \otimes [N_\nu]; [N-1, 1], [N-1]\{1\}(1)2; [1](1)(1)3; 1)$<br>$= (N(N-1))^{-1/2} \left( \sqrt{N_\nu(N_\pi-1)}  d_\pi f_\pi; 1\rangle - \sqrt{N_\pi(N_\nu-1)}  d_\nu f_\nu; 1\rangle \right)$  |

$$\begin{aligned}
& -N_\pi |d_\pi f_\nu; 1\rangle + N_\nu |d_\nu f_\pi; 1\rangle \\
|1_{\text{ms}}^{\prime\prime}\rangle &= |[N_\pi] \otimes [N_\nu]; [N-2, 2], [N-2, 1]\{1\}(1)2; [1](1)(1)3; 1) \\
&= ((N-1)(N-2))^{-1/2} \left( -\sqrt{N_\nu(N_\nu-1)} |d_\pi f_\pi; 1\rangle - \sqrt{N_\pi(N_\pi-1)} |d_\nu f_\nu; 1\rangle \right. \\
&\quad \left. + \sqrt{(N_\pi-1)(N_\nu-1)} |d_\pi f_\nu; 1\rangle + \sqrt{(N_\pi-1)(N_\nu-1)} |d_\nu f_\pi; 1\rangle \right) \\
|2_1^-\rangle &= |[N_\pi] \otimes [N_\nu]; [N], [N-1]\{1\}(1)2; [1](1)(1)3; 2) \\
&= (N(N-1))^{-1/2} \left( \sqrt{N_\pi(N_\pi-1)} |d_\pi f_\pi; 2\rangle + \sqrt{N_\nu(N_\nu-1)} |d_\nu f_\nu; 2\rangle \right. \\
&\quad \left. + \sqrt{N_\nu N_\pi} |d_\pi f_\nu; 2\rangle + \sqrt{N_\nu N_\pi} |d_\nu f_\pi; 2\rangle \right) \\
|3_2^-\rangle &= |[N_\pi] \otimes [N_\nu]; [N], [N-1]\{1\}(1)2; [1](1)(1)3; 3) \\
&= (N(N-1))^{-1/2} \left( \sqrt{N_\pi(N_\pi-1)} |d_\pi f_\pi; 3\rangle + \sqrt{N_\nu(N_\nu-1)} |d_\nu f_\nu; 3\rangle \right. \\
&\quad \left. + \sqrt{N_\nu N_\pi} |d_\pi f_\nu; 3\rangle + \sqrt{N_\nu N_\pi} |d_\nu f_\pi; 3\rangle \right) \\
|4_1^-\rangle &= |[N_\pi] \otimes [N_\nu]; [N], [N-1]\{1\}(1)2; [1](1)(1)3; 4) \\
&= (N(N-1))^{-1/2} \left( \sqrt{N_\pi(N_\pi-1)} |d_\pi f_\pi; 4\rangle + \sqrt{N_\nu(N_\nu-1)} |d_\nu f_\nu; 4\rangle \right. \\
&\quad \left. + \sqrt{N_\nu N_\pi} |d_\pi f_\nu; 4\rangle + \sqrt{N_\nu N_\pi} |d_\nu f_\pi; 4\rangle \right) \\
|5_1^-\rangle &= |[N_\pi] \otimes [N_\nu]; [N], [N-1]\{1\}(1)2; [1](1)(1)3; 5) \\
&= (N(N-1))^{-1/2} \left( \sqrt{N_\pi(N_\pi-1)} |d_\pi f_\pi; 5\rangle + \sqrt{N_\nu(N_\nu-1)} |d_\nu f_\nu; 5\rangle \right. \\
&\quad \left. + \sqrt{N_\nu N_\pi} |d_\pi f_\nu; 5\rangle + \sqrt{N_\nu N_\pi} |d_\nu f_\pi; 5\rangle \right)
\end{aligned}$$

TABLE II. Notation for some low-lying states in the  $\text{SO}_{\pi\nu}(6) \otimes \text{U}_{\pi\nu}(7)$  dynamical symmetry limit.

| $[[N_\pi] \otimes [N_\nu]; [N_1, N_2], [n_1, n_2] \langle \sigma_1, \sigma_2 \rangle (\tau_1, \tau_2) \{ \alpha_i \} L_d; [m_1, m_2] (\omega_1, \omega_2) (u_1, u_2) \{ \beta_j \} L_f; LM)$ |
|--|
| $ 0_1^+\rangle =  [N_\pi] \otimes [N_\nu]; [N], [N] \langle N \rangle (0)0; [0](0)(0)0; 0)$  |
| $ 0_2^+\rangle =  [N_\pi] \otimes [N_\nu]; [N], [N] \langle N \rangle (2)0; [0](0)(0)0; 0)$  |
| $ 1_{\text{ms}}^+\rangle =  [N_\pi] \otimes [N_\nu]; [N-1, 1], [N-1, 1] \langle N-1, 1 \rangle (1, 1)1; [0](0)(0)0; 1)$  |
| $ 2_1^+\rangle =  [N_\pi] \otimes [N_\nu]; [N], [N] \langle N \rangle (1)2; [0](0)(0)0; 2)$  |
| $ 2_2^+\rangle =  [N_\pi] \otimes [N_\nu]; [N], [N] \langle N \rangle (2)2; [0](0)(0)0; 2)$  |
| $ 2_{\text{ms}}^+\rangle =  [N_\pi] \otimes [N_\nu]; [N-1, 1], [N-1, 1] \langle N-1, 1 \rangle (1)2; [0](0)(0)0; 2)$   |
| $ 3_{\text{ms}}^+\rangle =  [N_\pi] \otimes [N_\nu]; [N-1, 1], [N-1, 1] \langle N-1, 1 \rangle (1, 1)3; [0](0)(0)0; 3)$  |
| $ 4_1^+\rangle =  [N_\pi] \otimes [N_\nu]; [N], [N] \langle 2 \rangle (2)4; [0](0)(0)0; 4)$  |
| $ 3_1^-\rangle =  [N_\pi] \otimes [N_\nu]; [N], [N-1] \langle N-1 \rangle (0)0; [1](1)(1)3; 3)$  |
| $ 3_{\text{ms}}^{\prime-}\rangle =  [N_\pi] \otimes [N_\nu]; [N-1, 1], [N-1] \langle N-1 \rangle (0)0; [1](1)(1)3; 3)$   |
| $ 1_1^-\rangle =  [N_\pi] \otimes [N_\nu]; [N], [N-1] \langle N-1 \rangle (1)2; [1](1)(1)3; 1)$  |
| $ 1_{\text{ms}}^-\rangle =  [N_\pi] \otimes [N_\nu]; [N-1, 1], [N-2, 1] \langle N-2, 1 \rangle (1)2; [1](1)(1)3; 1)$   |
| $ 1_{\text{ms}}^{\prime-}\rangle =  [N_\pi] \otimes [N_\nu]; [N-1, 1], [N-1] \langle N-1 \rangle (1)2; [1](1)(1)3; 1)$   |
| $ 1_{\text{ms}}^{\prime\prime-}\rangle =  [N_\pi] \otimes [N_\nu]; [N-2, 2], [N-2, 1] \langle N-2, 1 \rangle (1)2; [1](1)(1)3; 1)$   |

TABLE III. Some analytical expressions for reduced electromagnetic transition strengths in the  $U_{\pi\nu}(1) \otimes U_{\pi\nu}(5) \otimes U_{\pi\nu}(7)$  dynamical symmetry limit.

---



---


$$B(E3; 0_1^+ \rightarrow 3_1^-) = 7e_3^2 N$$


---


$$B(E1; 3_1^- \rightarrow 2_1^+) = \frac{3}{7} \left[ (\alpha_\nu N_\nu + \alpha_\pi N_\pi) \frac{1}{N} + \beta (N_\pi + \eta N_\nu) \frac{2N-1}{2N^2} + \sqrt{\frac{6}{35}} \beta \chi (\chi_\pi N_\pi + \chi_\nu \eta N_\nu) \frac{1}{N^2} \right]^2$$

$$B(E1; 3_1^- \rightarrow 2_{ms}^+) = \frac{3}{7} \left[ \alpha_\pi - \alpha_\nu + \beta (1 - \eta) \frac{2N-1}{2N} + \sqrt{\frac{6}{35}} \beta \chi (\chi_\pi - \eta \chi_\nu) \frac{1}{N} \right]^2 \frac{N_\nu N_\pi}{N^2}$$

$$B(E1; 1_1^- \rightarrow 0_1^+) = \beta^2 (N_\pi + \eta N_\nu)^2 \frac{N-1}{N^3}$$

$$B(E1; 1_1^- \rightarrow 2_1^+) = \frac{6}{25} \beta^2 \left[ \chi (N_\pi + \eta N_\nu) + \sqrt{\frac{5}{42}} (\chi_\pi N_\pi + \eta \chi_\nu N_\nu) \right]^2 \frac{N-1}{N^4}$$

$$B(E1; 1_1^- \rightarrow 0_2^+) = \frac{2}{5} \left[ (\alpha_\nu N_\nu + \alpha_\pi N_\pi) \frac{1}{N} + \beta (N_\pi + \eta N_\nu) \frac{2N-3}{2N^2} + 3 \sqrt{\frac{6}{35}} \beta \chi (\chi_\pi N_\pi + \eta \chi_\nu N_\nu) \frac{1}{N^2} \right]^2$$

$$B(E1; 1_1^- \rightarrow 2_2^+) = \frac{2}{35} \left[ (\alpha_\nu N_\nu + \alpha_\pi N_\pi) \frac{1}{N} - \beta (N_\pi + \eta N_\nu) \frac{2N-3}{2N^2} - \sqrt{\frac{6}{35}} \beta \chi (\chi_\pi N_\pi + \eta \chi_\nu N_\nu) \frac{1}{N^2} \right]^2$$

$$B(E1; 4_1^- \rightarrow 4_1^+) = \frac{1}{7} \left[ (\alpha_\nu N_\nu + \alpha_\pi N_\pi) \frac{1}{N} + \beta (N_\pi + \eta N_\nu) \frac{2N-3}{2N^2} + 3 \sqrt{\frac{6}{35}} \beta \chi (\chi_\pi N_\pi + \eta \chi_\nu N_\nu) \frac{1}{N^2} \right]^2$$

$$B(E1; 5_1^- \rightarrow 4_1^+) = \frac{6}{7} \left[ (\alpha_\nu N_\nu + \alpha_\pi N_\pi) \frac{1}{N} + \beta (N_\pi + \eta N_\nu) \frac{2N-3}{2N^2} + 4 \sqrt{\frac{2}{105}} \beta \chi (\chi_\pi N_\pi + \eta \chi_\nu N_\nu) \frac{1}{N^2} \right]^2$$

$$B(E1; 3_1^- \rightarrow 4_1^+) = \frac{3}{245} \beta^2 \chi^2 (N_\pi + \eta N_\nu)^2 \frac{N-1}{N^4}$$

$$B(E1; 3_1^- \rightarrow 2_2^+) = \frac{144}{245} \beta^2 \chi^2 (N_\pi + \eta N_\nu)^2 \frac{N-1}{N^4}$$

$$B(E1; 4_1^- \rightarrow 3_1^+) = \frac{289}{280} \beta^2 \chi^2 (N_\pi + \eta N_\nu)^2 \frac{N-2}{N^4}$$

$$B(E1; 5_1^- \rightarrow 6_1^+) = \frac{13}{385} \beta^2 \chi^2 (N_\pi + \eta N_\nu)^2 \frac{N-2}{N^4}$$

$$B(E2; 1_{ms}^- \rightarrow 3_1^-) = (e_\pi - e_\nu)^2 \frac{N_\pi N_\nu (N-2)}{N(N-1)}$$

$$B(M1; 1_{ms}^- \rightarrow 1_1^-) = \frac{3}{2\pi} (g_\pi - g_\nu)^2 \frac{N_\pi N_\nu (N-2)}{N(N-1)^2}$$

$$B(M1; 1_{ms}^- \rightarrow 2_1^-) = \frac{3}{\pi} (g_\pi - g_\nu)^2 \frac{N_\pi N_\nu (N-2)}{N(N-1)^2}$$

$$B(E1; 1_{ms}^- \rightarrow 0_1^+) = \beta^2 (1 - \eta)^2 \frac{N_\pi N_\nu (N-2)}{N^2(N-1)}$$

$$B(M1; 3_{ms}^- \rightarrow 3_1^-) = \frac{9}{\pi} (g'_\pi - g'_\nu)^2 \frac{N_\pi N_\nu}{N^2}$$

$$B(E1; 3_{ms}^- \rightarrow 2_1^+) = \frac{3}{7} \left[ \alpha_\pi - \alpha_\nu - \frac{1}{2} \beta (1 - \eta) \frac{1}{N} + \sqrt{\frac{6}{35}} \beta \chi (\chi_\pi - \eta \chi_\nu) \frac{1}{N} \right]^2 \frac{N_\pi N_\nu}{N^2}$$

$$B(E1; 3_{ms}^- \rightarrow 2_{ms}^+) = \frac{3}{7} \left[ (\alpha_\pi N_\pi + \alpha_\nu N_\nu) - \frac{1}{2} \beta (N_\nu + \eta N_\pi) \frac{1}{N} + \sqrt{\frac{6}{35}} \beta \chi (\chi_\pi N_\nu + \eta \chi_\nu N_\pi) \frac{1}{N} \right]^2 \frac{1}{N^2}$$

$$B(E2; 1_{ms}'^- \rightarrow 3_1^-) = (e_\pi - e_\nu)^2 \frac{N_\pi N_\nu}{N^2(N-1)}$$

$$B(M1; 1_{ms}'^- \rightarrow 1_1^-) = \frac{3}{2\pi} \left[ \frac{g_\pi - g_\nu}{N-1} - 2(g'_\pi - g'_\nu) \right]^2 \frac{N_\pi N_\nu}{N^2}$$

$$B(M1; 1_{ms}'^- \rightarrow 2_1^-) = \frac{3}{\pi} \left[ \frac{g_\pi - g_\nu}{N-1} - (g'_\pi - g'_\nu) \right]^2 \frac{N_\pi N_\nu}{N^2}$$

$$B(E1; 1_{ms}'^- \rightarrow 0_1^+) = \beta^2 (1 - \eta)^2 \frac{N_\pi N_\nu}{N^3(N-1)}$$

$$B(E1; 1_{ms}'^- \rightarrow 2_1^+) = \frac{1}{35} \beta^2 \left[ \chi_\pi - \eta \chi_\nu + \sqrt{\frac{42}{5}} (1 - \eta) \chi \right]^2 \frac{N_\pi N_\nu}{N^4(N-1)}$$


---



---

TABLE IV. Some analytical expressions for reduced electromagnetic transition strengths in the  $SO_{\pi\nu}(6) \otimes U_{\pi\nu}(7)$  dynamical symmetry limit.

|                                     |   |   |
|-------------------------------------|---|---|
| $B(E3; 0_1^+ \rightarrow 3_1^-)$    | = | $\frac{7}{2} e_3^2 \frac{N(N+3)}{N+1}$  |
| $B(E1; 3_1^- \rightarrow 2_1^+)$    | = | $\frac{3}{70} \left[ \alpha_\nu N_\nu + \alpha_\pi N_\pi + \beta (N_\pi + \eta N_\nu) \frac{2N-1}{2N} \right]^2 \frac{(N+3)(N+4)}{N^2(N+1)}$                              |
| $B(E1; 2_{ms}^+ \rightarrow 3_1^-)$ | = | $\frac{3}{35} \left[ 2(\alpha_\pi - \alpha_\nu) \frac{N+1}{N+2} + \beta(1-\eta) \left( 1 - \frac{N+1}{N(N+2)} \right) \right]^2 \frac{(N+2)(N+3)N_\nu N_\pi}{N^2(N+1)^2}$ |
| $B(E1; 1_1^- \rightarrow 0_1^+)$    | = | $\frac{1}{10} \left[ \alpha_\nu N_\nu + \alpha_\pi N_\pi + \beta (N_\pi + \eta N_\nu) \frac{2N+7}{2N} \right]^2 \frac{N-1}{N(N+1)}$                                       |
| $B(E1; 1_1^- \rightarrow 2_1^+)$    | = | $\frac{3}{1225} \beta^2 \chi^2 (N_\pi + \eta N_\nu)^2 \frac{(N-1)(N+4)(N+5)^2}{N^4(N+1)}$   |

TABLE V. Some experimental and theoretical transition strengths for  $^{142}\text{Ce}$ . The parameters of the transition operators used for the calculation are specified in the text. The asterisks denote transition strengths, which were used to fit the model parameters as discussed in the text.

|                                       | Experiment [16]  | Theory I                            | Theory II                           |
|---------------------------------------|--|-------------------------------------|-------------------------------------|
| $B(E3; 0_1^+ \rightarrow 3_1^-)$ *    | $2.02_{-0.13}^{+0.13} \times 10^5 e^2\text{fm}^6$      | $2.02 \times 10^5 e^2\text{fm}^6$   | $2.02 \times 10^5 e^2\text{fm}^6$   |
| $B(E1; 3_1^- \rightarrow 2_1^+)$ *    | $< 2.1 \times 10^{-4} e^2\text{fm}^2$                  | $1.0 \times 10^{-4} e^2\text{fm}^2$ | $1.0 \times 10^{-4} e^2\text{fm}^2$ |
| $B(E1; 3_1^- \rightarrow 4_1^+)$      | $< 3.9 \times 10^{-3} e^2\text{fm}^2$                  | $4.3 \times 10^{-4} e^2\text{fm}^2$ | $4.7 \times 10^{-4} e^2\text{fm}^2$ |
| $B(E1; 3_1^- \rightarrow 2_2^+)$      |  | $2.1 \times 10^{-2} e^2\text{fm}^2$ | $2.3 \times 10^{-2} e^2\text{fm}^2$ |
| $B(E1; 2_{ms}^+ \rightarrow 3_1^-)$ * | $4.6_{-0.5}^{+0.5} \times 10^{-3} e^2\text{fm}^2$      | $4.6 \times 10^{-3} e^2\text{fm}^2$ | $4.6 \times 10^{-3} e^2\text{fm}^2$ |
| $B(E1; 4_1^- \rightarrow 3_1^+)$      | $4.4_{-2.5}^{+3.7} \times 10^{-2} e^2\text{fm}^2$      | $2.7 \times 10^{-2} e^2\text{fm}^2$ | $3.0 \times 10^{-2} e^2\text{fm}^2$ |
| $B(E1; 4_1^- \rightarrow 4_1^+)$      | $7.4_{-4.6}^{+7.0} \times 10^{-4}$                     | $1.7 \times 10^{-4} e^2\text{fm}^2$ | $5.8 \times 10^{-4} e^2\text{fm}^2$ |
| $B(E1; 5_1^- \rightarrow 4_1^+)$      | $< 1.2 \times 10^{-3} e^2\text{fm}^2$                  | $3.8 \times 10^{-5} e^2\text{fm}^2$ | $1.0 \times 10^{-3} e^2\text{fm}^2$ |
| $B(E1; 5_1^- \rightarrow 6_1^+)$      | $< 1.7 \times 10^{-3} e^2\text{fm}^2$                  | $8.9 \times 10^{-4} e^2\text{fm}^2$ | $9.7 \times 10^{-4} e^2\text{fm}^2$ |
| $B(E1; 1_1^- \rightarrow 0_1^+)$ *    | $3.9_{-1.2}^{+1.2} \times 10^{-3} e^2\text{fm}^2$ [54] | $3.9 \times 10^{-3} e^2\text{fm}^2$ | $3.9 \times 10^{-3} e^2\text{fm}^2$ |
| $B(E1; 1_1^- \rightarrow 2_1^+)$ *    | $8.9_{-3.3}^{+3.3} \times 10^{-3} e^2\text{fm}^2$ [54] | $8.9 \times 10^{-3} e^2\text{fm}^2$ | $8.9 \times 10^{-3} e^2\text{fm}^2$ |
| $B(E1; 1_1^- \rightarrow 0_2^+)$      |  | $4.8 \times 10^{-4} e^2\text{fm}^2$ | $1.7 \times 10^{-3} e^2\text{fm}^2$ |
| $B(E1; 1_1^- \rightarrow 2_2^+)$      |  | $6.0 \times 10^{-5} e^2\text{fm}^2$ | $2.1 \times 10^{-6} e^2\text{fm}^2$ |
| $B(E1; 3_1^+ \rightarrow 3_1^-)$      | $4.4_{-3.0}^{+3.3} \times 10^{-4} e^2\text{fm}^2$      | 0                                   | 0                                   |
| $B(E2; 1_{ms}^- \rightarrow 3_1^-)$   |  | $86.4 e^2\text{fm}^4$               | $86.4 e^2\text{fm}^4$               |
| $B(M1; 1_{ms}^- \rightarrow 1_1^-)$   |  | $0.072 \mu_N^2$                     | $0.072 \mu_N^2$                     |
| $B(M1; 1_{ms}^- \rightarrow 2_1^-)$   |  | $0.143 \mu_N^2$                     | $0.143 \mu_N^2$                     |
| $B(E1; 1_{ms}^- \rightarrow 0_1^+)$   |  | $4.0 \times 10^{-4} e^2\text{fm}^2$ | $4.0 \times 10^{-4} e^2\text{fm}^2$ |
| $B(E2; 1_{ms}' \rightarrow 3_1^-)$    |  | $5.8 e^2\text{fm}^4$                | $5.8 e^2\text{fm}^4$                |
| $B(M1; 1_{ms}' \rightarrow 1_1^-)$    |  | $0.005 \mu_N^2$                     | $0.005 \mu_N^2$                     |
| $B(M1; 1_{ms}' \rightarrow 2_1^-)$    |  | $0.01 \mu_N^2$                      | $0.01 \mu_N^2$                      |
| $B(E1; 1_{ms}' \rightarrow 0_1^+)$    |  | $2.7 \times 10^{-5} e^2\text{fm}^2$ | $2.7 \times 10^{-5} e^2\text{fm}^2$ |
| $B(E1; 1_{ms}' \rightarrow 2_1^+)$    |  | $2.7 \times 10^{-4} e^2\text{fm}^2$ | $2.2 \times 10^{-4} e^2\text{fm}^2$ |

TABLE VI. Some experimental and theoretical transition strengths for  $^{94}\text{Mo}$ .

|  | Experiment  | Theory                                      |
|--|---|---|
| $B(E3; 0_1^+ \rightarrow 3_1^-)$           | $6.2_{-1.2}^{+1.2} \times 10^4 \text{ e}^2\text{fm}^6{}^{\text{a}}$                                   | $6.2 \times 10^4 \text{ e}^2\text{fm}^6$    |
| $B(M1; 0_1^+ \rightarrow 1_1^+)$           | $0.48(3) \mu_N^2{}^{\text{b}}$  | $0.48 \mu_N^2$                              |
| $B(M1; 1_1^+ \rightarrow 2_1^+)$           | $0.007_{-2}^{+6} \mu_N^2{}^{\text{b}}$  | $0 \mu_N^2$                                 |
| $B(M1; 1_1^+ \rightarrow 2_2^+)$           | $0.43(5) \mu_N^2{}^{\text{b}}$  | $0.36 \mu_N^2$                              |
| $B(M1; 2_{\text{ms}}^+ \rightarrow 2_1^+)$ | $0.48(6) \mu_N^2{}^{\text{b}}$  | $0.30 \mu_N^2$                              |
| $B(E1; 3_1^- \rightarrow 2_1^+)$           | $0.14 \times 10^{-4} \text{ e}^2\text{fm}^2 - 1.0 \times 10^{-4} \text{ e}^2\text{fm}^2{}^{\text{c}}$ | $0.4 \times 10^{-4} \text{ e}^2\text{fm}^2$ |
| $B(E1; 3_1^- \rightarrow 2_{\text{ms}}^+)$ | $1.0 \times 10^{-4} \text{ e}^2\text{fm}^2 - 6.0 \times 10^{-4} \text{ e}^2\text{fm}^2{}^{\text{c}}$  | $5.8 \times 10^{-4} \text{ e}^2\text{fm}^2$ |
| $B(E1; 1_1^- \rightarrow 0_1^+)$           | $3.3_{-1.7}^{+1.7} \times 10^{-4} \text{ e}^2\text{fm}^2{}^{\text{d}}$                                | $3.2 \times 10^{-4} \text{ e}^2\text{fm}^2$ |
| $B(E1; 1_1^- \rightarrow 2_1^+)$           | $5.6_{-3.5}^{+3.5} \times 10^{-4} \text{ e}^2\text{fm}^2{}^{\text{d}}$                                | $5.5 \times 10^{-4} \text{ e}^2\text{fm}^2$ |

<sup>a</sup>from Ref. [59].

<sup>b</sup>from Ref. [31].

<sup>c</sup>from Ref. [36].

<sup>d</sup>from Ref. [55].

TABLE VII. Partial classification scheme for the chain  $U_{\pi\nu}(7) \supset SO_{\pi\nu}(7) \supset G_{2\pi\nu} \supset SO_{\pi\nu}(3)$ 

| $U_{\pi\nu}(7)$ | $SO_{\pi\nu}(7)$       | $G_{2\pi\nu}$ | $SO_{\pi\nu}(3)$  |
|-----------------|------------------------|---------------|---|
| $[m_1, m_2]$    | $(\omega_1, \omega_2)$ | $(u_1, u_2)$  | $L$   |
| [1]             | (1, 0)                 | (1, 0)        | 3   |
| [2]             | (2, 0)                 | (2, 0)        | 2,4,6   |
|                 | (0, 0)                 | (0, 0)        | 0   |
| [1, 1]          | (1, 1)                 | (1, 0)        | 3   |
|                 |                        | (1, 1)        | 1,5   |
| [3]             | (3, 0)                 | (3, 0)        | 1,3,4,5,6,7,9   |
|                 | (1, 0)                 | (1, 0)        | 3   |
| [2, 1]          | (1, 0)                 | (1, 0)        | 3   |
|                 | (2, 1)                 | (2, 0)        | 2,4,6   |
|                 |                        | (2, 1)        | 2,3,4,5,7,8   |
|                 |                        | (1, 1)        | 1,5   |
| [4]             | (4, 0)                 | (4, 0)        | 0, 2, 3, 4 <sup>2</sup> , 5, 6 <sup>2</sup> , 7, 8 <sup>2</sup> , 9, 10, 12               |
|                 | (2, 0)                 | (2, 0)        | 2,4,6   |
| [3, 1]          | (2, 0)                 | (2, 0)        | 2,4,6   |
|                 | (3, 1)                 | (3, 0)        | 1,3,4,5,6,7,9   |
|                 |                        | (3, 1)        | 1, 2, 3 <sup>2</sup> , 4, 5 <sup>2</sup> , 6 <sup>2</sup> , 7 <sup>2</sup> , 8, 9, 10, 11 |
|                 |                        | (2, 1)        | 2,3,4,5,7,8   |
|                 | (1, 1)                 | (1, 0)        | 3   |
|                 |                        | (1, 1)        | 1,5   |
| [2, 2]          | (2, 0)                 | (2, 0)        | 2,4,6   |
|                 | (0, 0)                 | (0, 0)        | 0   |
|                 | (2, 2)                 | (2, 0)        | 2,4,6   |
|                 |                        | (2, 2)        | 0,2,4,5,6,8,10  |
|                 |                        | (2, 1)        | 2,3,4,5,7,8   |

FIGURES

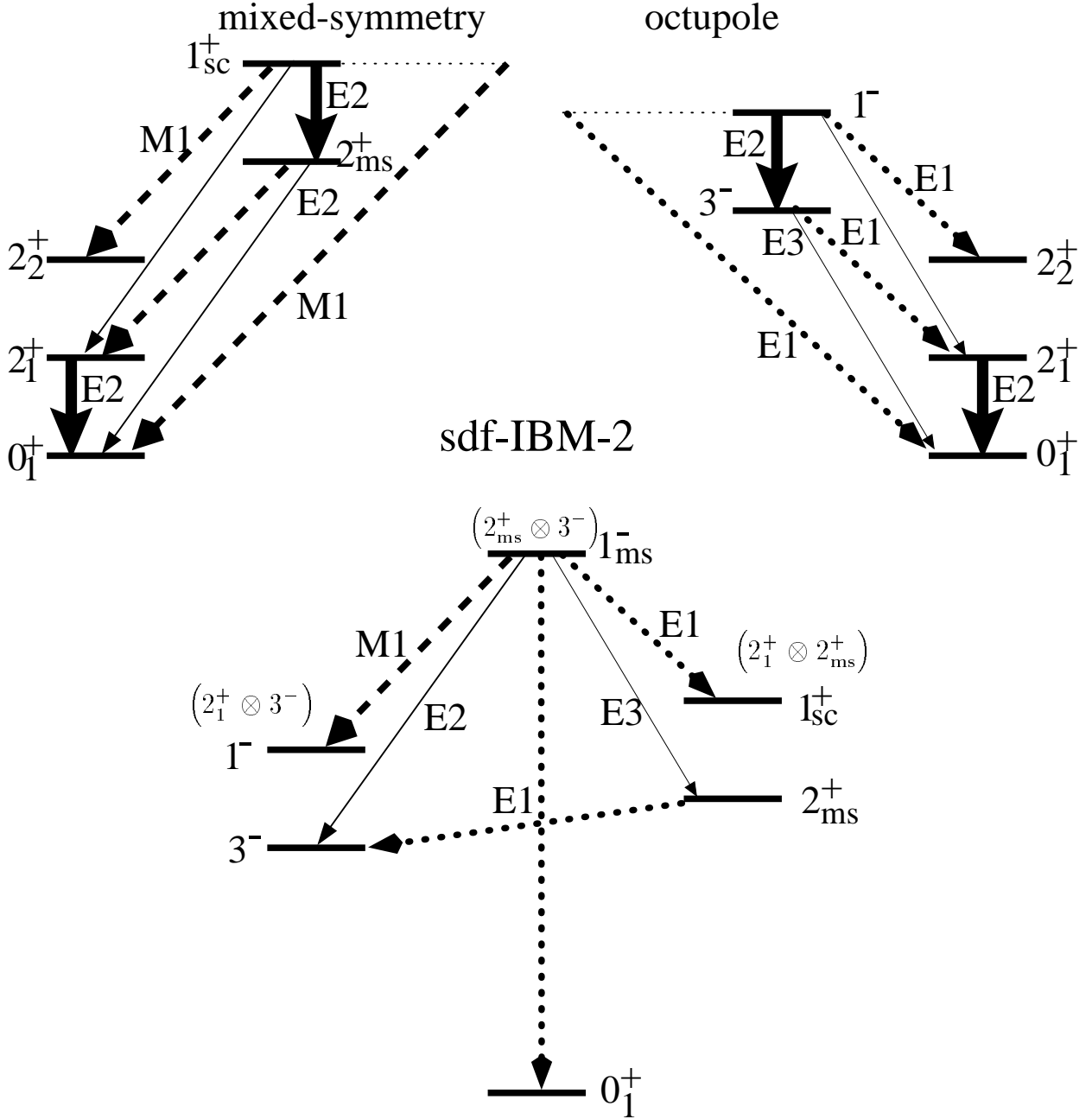


FIG. 1. Expected decays of fundamental one-phonon and two-phonon states in the *sdf*-IBM-2.  $2_{ms}^+ \rightarrow 3^-$  transitions were observed already experimentally [16,36].

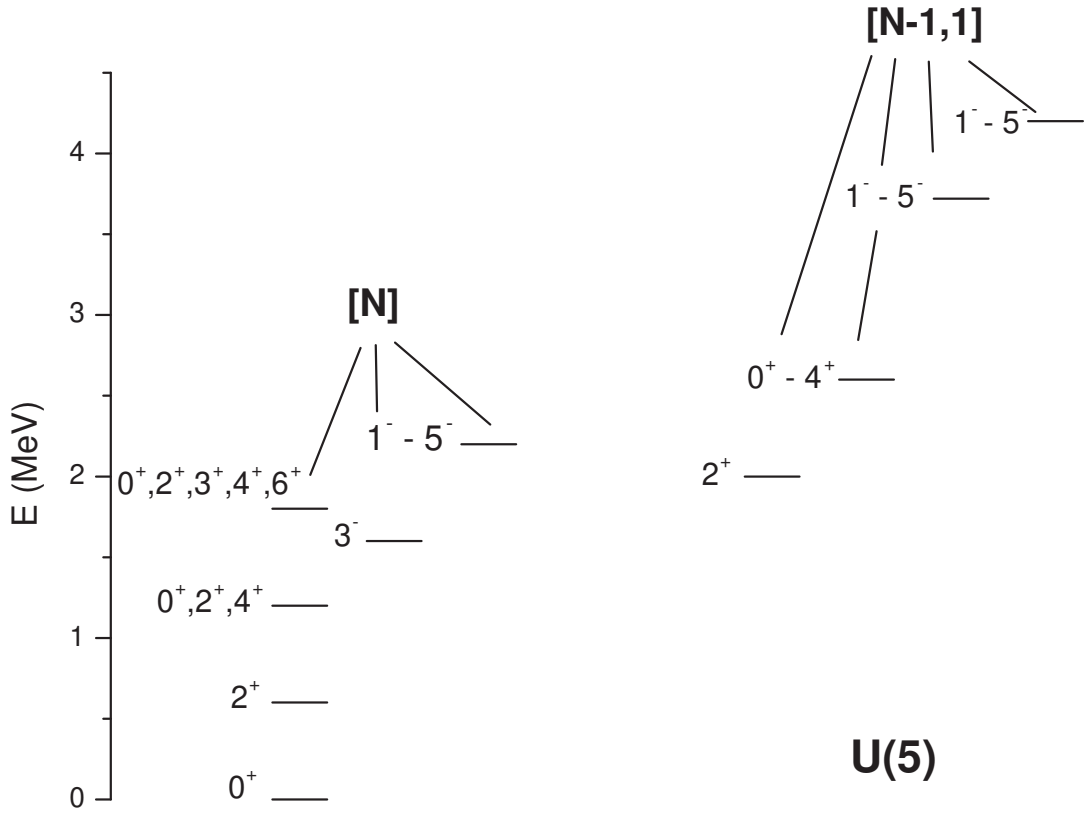


FIG. 2. Sketch of the relevant low-energy spectrum in the  $U(5) \otimes U(7)$  dynamical symmetry limit calculated for five bosons ( $N_\pi = 4$ ,  $N_\nu = 1$ ) with the set of parameters:  $\epsilon_d = 0.6$  MeV,  $\epsilon_f = 1.6$  MeV,  $\lambda = 0.4$  MeV and  $\lambda' = -0.12$  MeV. The other parameters from Eq. (20) are put equal to 0.

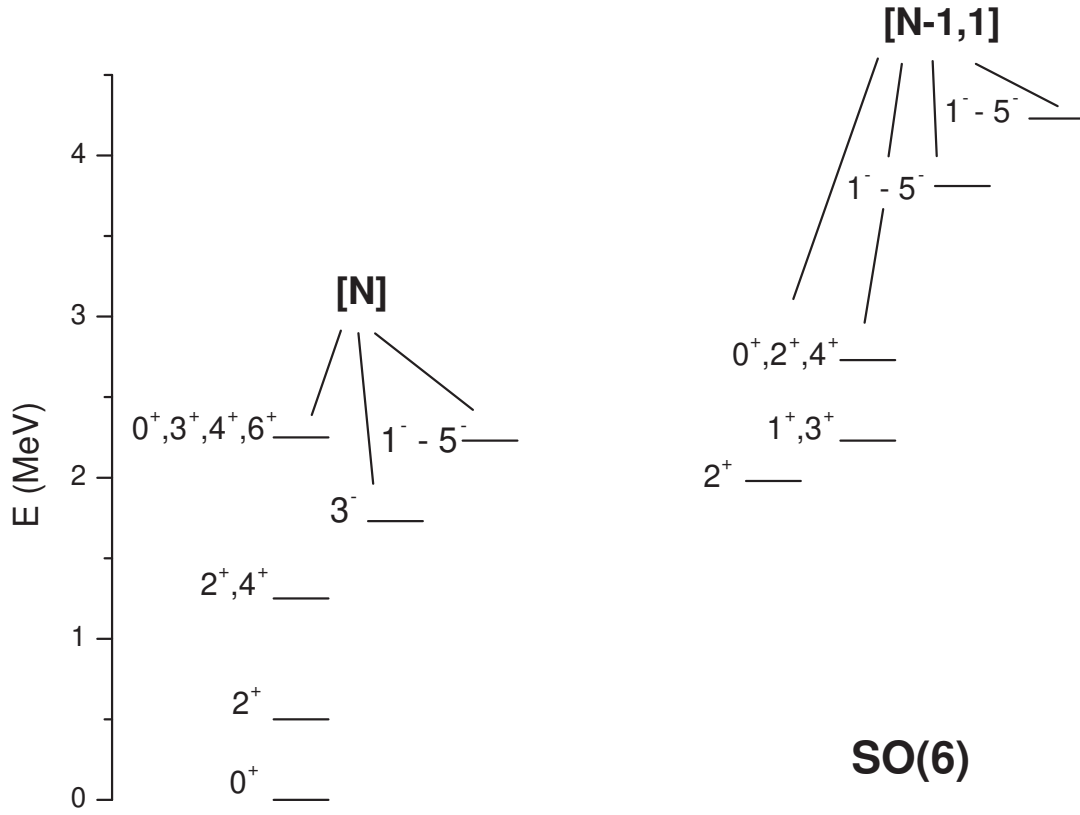


FIG. 3. Sketch of the relevant low-energy spectrum in the  $SO(6) \otimes U(7)$  dynamical symmetry limit with the set of parameters:  $\zeta = -0.01$  MeV,  $\beta = 0.125$  MeV,  $\epsilon_f = 1.6$  MeV,  $\lambda = 0.4$  MeV,  $\lambda' = -0.12$  MeV and  $H_0 = 0.45$  MeV (the other parameters from (24) are equal to 0) and  $N_\pi = 4$ ,  $N_\nu = 1$ .